

# COMPUTATIONAL MODELING OF HUMAN HEAD TO STUDY TRAUMATIC BRAIN INJURY

A DISSERTATION

*Submitted in partial fulfillment of the  
Requirements for the award of the degree*

*of*

MASTER OF TECHNOLOGY

*in*

MECHANICAL ENGINEERING

**(With Specialization in Machine Design Engineering)**

*by*

**DEEPAK SHARMA**



**DEPARTMENT OF MECHANICAL AND INDUSTRIAL ENGINEERING  
INDIAN INSTITUTE OF TECHNOLOGY ROORKEE  
ROORKEE-247667 (INDIA)**



# INDIAN INSTITUTE OF TECHNOLOGY ROORKEE, ROORKEE

## CANDIDATE'S DECLARATION

I hereby declare that the work carried out in this report entitled “**Computational Modeling Of Human Head To Study Traumatic Brain Injury**”, is presented on behalf of partial fulfillment of the requirement for the Dissertation of “ **Master of Technology**” in Mechanical Engineering with specialization in **Machine Design Engineering** submitted to Department of Mechanical and Industrial Engineering, Indian Institute of Technology Roorkee under the supervision of **Dr. S. G. GANPULE**, Assistant professor, Department of Mechanical and Industrial Engineering, Indian Institute of Technology Roorkee.

Date:

Place: Roorkee

(**Deepak Sharma**)

## **CERTIFICATE**

This is to certify that the above statement made by the candidate is correct to the best of my knowledge and belief.

**(Dr. S.G. GANPULE)**  
Assistant Professor  
MIED, IIT Roorkee  
(Supervisor)

**(Dr. A.K. SWAIN)**  
Assistant Professor  
MIED, IIT Roorkee  
(Co-Guide)



## ABSTRACT

Traumatic brain injury (TBI) is a major health concern, conservative estimates indicate that nearly 1.6 million people suffer from TBI annually in India. Road traffic accidents and falls are identified as the leading causes of TBI among the Indian population. Knowledge of brain deformations during accelerative or impact loading is critical for the overall management of TBI, including the development of injury thresholds and personal protective equipment. Current helmets provide considerable protection against the linear impact (acceleration), whereas their protection against the rotational accelerations is unclear. Recent investigations suggest that rotational acceleration induced due to rotation of the head is more deleterious than the linear acceleration in causing TBI. Current helmets are neither designed nor tested for rotational loading. During this research, we propose to study mechanics of head rotation under impact loading conditions. We specifically define following two objectives (i) to study the brain biomechanics under rotational loading. (ii) To study the effectiveness of the helmets and different types of foam pads in mitigating head acceleration.

A better understanding of mechanics of impact induced injury will enable us to determine the critical parameters that causes brain injury which can lead to reduction in mortality rate in accidents. In normal daily life activities simple movements of body lead to small deformation of brain. When an external object hit the head like punching a boxer or heading a football, severe injuries can occur due to irreversible effects in neural, axonal and vascular structures of the brain. So to identify the deformations during rapid angular acceleration we have done our simulation study with 2 and 3 dimensional models. The effect of helmet is found positive in almost all cases except it increases the rotational acceleration.

## ACKNOWLEDGEMENTS

I wish to express a deep sense of gratitude and sincere thanks to my supervisor Dr. S.G. Ganpule and Dr. A.K. Swain, Department of Mechanical and Industrial Engineering, Indian Institute of Technology, Roorkee for their invaluable inspiration, wholehearted co-operation, motivation and important assistances throughout the duration. I consider myself fortunate to have had the opportunity to work under their able guidance and enrich myself from their depths of knowledge.

I would like to especially thank Mr. Sunil Sutar and Mr. Abhilash Singh, Ph.D. Scholars for their valuable cooperation, suggestions, help and guidance in my project work.

I take this opportunity to put on records my respects to Professor Dr. B. K. Gandhi, HOD Department of Mechanical and Industrial Engineering, Indian Institute of Technology Roorkee, for providing various facilities during course of present investigation.

Deepak sharma

Enrollment No: 17539003

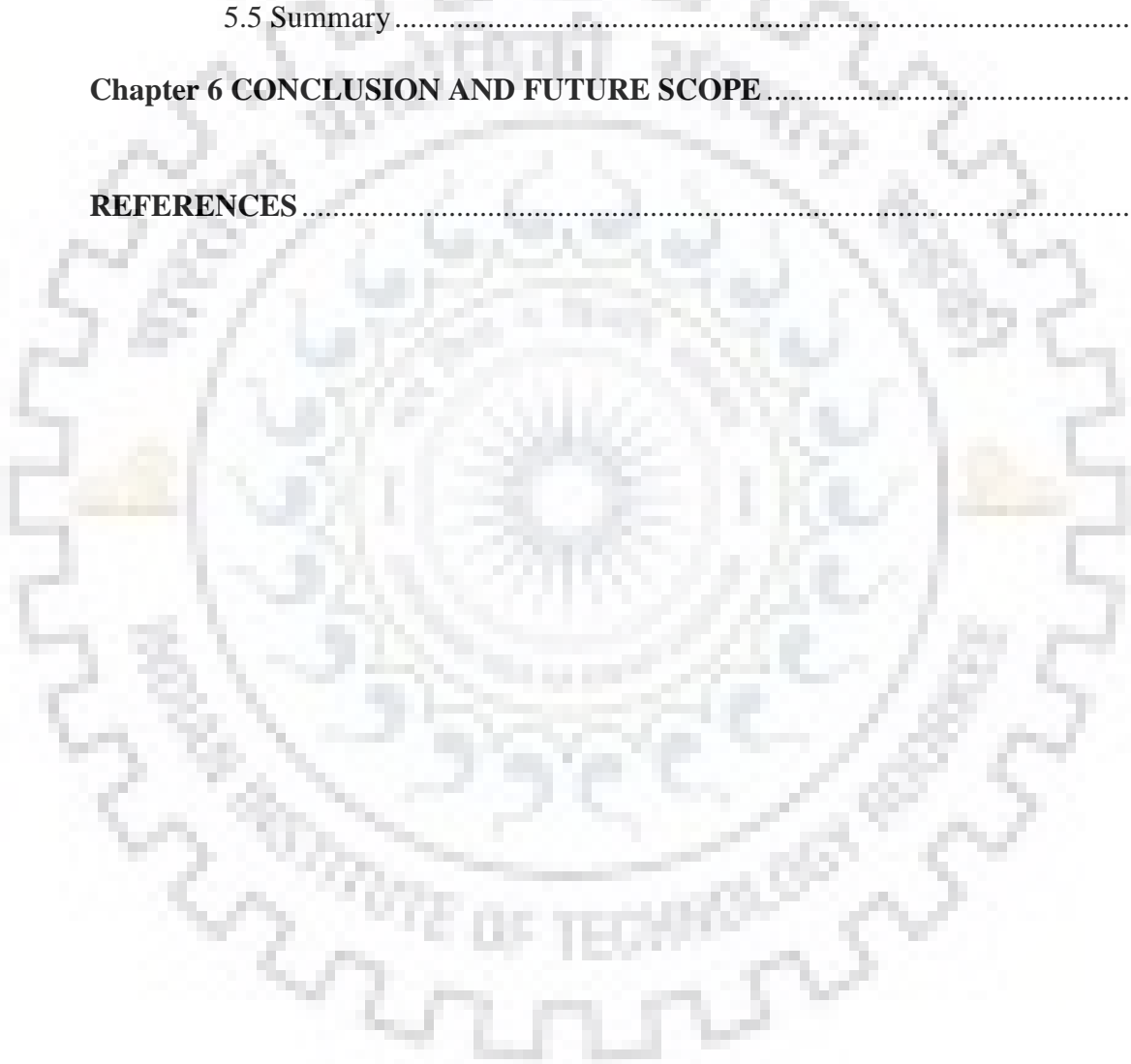
M. Tech (Machine Design Engineering)

MIED, IIT Roorkee

## TABLE OF CONTENT

<b>Title</b>	<b>Page</b>
<b>CANDIDATE’S DECLARATION</b> .....	<b>ii</b>
<b>ABSTRACT</b> .....	<b>iv</b>
<b>ACKNOWLEDGEMENTS</b> .....	<b>v</b>
<b>TABLE OF CONTENT</b> .....	<b>vi</b>
<b>LIST OF FIGURES</b> .....	<b>viii</b>
<b>LIST OF TABLES</b> .....	<b>x</b>
<b>Chapter 1 INTRODUCTION</b> .....	<b>1</b>
1.1 Traumatic Brain Injury .....	1
1.2 Mechanisms of Traumatic Brain Injury .....	2
1.2.1 Brain Injuries Induced by Rotational kinematics .....	2
1.2.2 Brain Injuries Induced by Linear kinematics .....	4
1.3 OBJECTIVE OF CURRENT WORK.....	4
<b>Chapter 2 LITERATURE REVIEW</b> .....	<b>6</b>
2.1 Finite Element Studies Review .....	6
2.2 Experimental Studies Review .....	8
4.4 Summary .....	11
<b>Chapter 3 METHODOLOGY</b> .....	<b>12</b>
3.1 Introduction.....	12
3.2 2-Dimensional Finite Element Model Description .....	12
3.3 Materials models .....	13
3.3.1 Viscoelastic Material Model .....	13
3.3.2 Hyperelastic Material Model .....	16
3.4 3-D Helmet and Foam Model .....	18
3.5 Hybrid III Human Dummy Model .....	21
3.6 GHBMC Full Body Model .....	23
3.7 Solution Scheme in Abaqus .....	24
3.8 Solution Scheme in Ls Dyna.....	25
3.9 Summary .....	25
<b>Chapter 4 VALIDATION OF MODEL</b> .....	<b>26</b>
4.1 Introduction.....	26
4.2 Load .....	26
4.3 Boundary Condition.....	26
4.4 Simulation Results .....	27

<b>Chapter 5 RESULTS AND DISCUSSION .....</b>	<b>30</b>
5.1 Introduction.....	30
5.2 Hybrid-III dummy Frontal Impact.....	30
5.2.1 Simulation Results Without Helmet Impact.....	32
5.2.2 Simulation Results with Helmet Impact.....	33
5.3 Simulations On Two Dimensional Model .....	35
5.3.1 Boundary conditions.....	35
5.3.2 Simulation Results.....	35
5.4 Simulations On GHBMC full body model .....	40
5.4.1 Simulation results for GHBMC full body model .....	42
5.5 Summary.....	44
<b>Chapter 6 CONCLUSION AND FUTURE SCOPE .....</b>	<b>45</b>
<b>REFERENCES .....</b>	<b>47</b>



## LIST OF FIGURES

---

Figure 1: Biomechanics of DAI and Contusions .....	3
Figure 2: Subdural hematoma.....	4
Figure 3: Front impact response of 2D head . Negative strains represent coup regions and positive strain contrecoup regions. [11] .....	7
Figure 4 :(a)Frontal impact (b)lateral intracranial pressure responses [14].....	8
Figure 5: Representative instrumentation x-rays showing the NDT clusters [20].....	10
Figure 6: (a)MRI scan of a human head in the mid-sagittal plane (b) 2D CAD model made in Solidworks. ....	12
Figure 7: FEM model with mesh and reference points.....	13
Figure 8: Stress-strain diagram for viscoelastic material at two different strain rates.....	14
Figure 9: Stress relaxation behaviour of viscoelastic material (a) initial applied strain (b)stress. ....	14
Figure 10: Creep in viscoelastic material (a)applied stress (b)corresponding strain with time.....	14
Figure 11: Shear relaxation curve .....	15
Figure 12: Stress-strain curve for linear elastic and hyperelastic material. ....	16
Figure 13: ACH helmet (a) shell (b) foam pad. ....	18
Figure 14:(a) ACH helmet with pad (b) FE model of ACH helmet. ....	19
Figure 15: Indicative stress-strain curve for foam material [25]. ....	19
Figure 16: Hysteresis curve for foam material [26].....	20
Figure 17: Uniaxial stress-strain curve for hard foam [28].....	21
Figure 18: (a)Hybrid III 50th Percentile Crash Test Dummy (b) Fast FE model of 50 <sup>th</sup> Hybrid III dummy [29].....	22
Figure 19: FE model of neck for Hybrid III dummy [29].....	22
Figure 20: Maximum flexion and extension of FE neck head assembly [29] .....	23
Figure 21: GHBMCM50 detailed Pedestrian full body model [30] .....	24
Figure 22: Profile of applied acceleration pulse and corresponding velocity.....	26
Figure 23:Reference point and constraint .....	27
Figure 24:Variation of shear strain inside the brain.....	28
Figure 25:Components of the Lagrangian strain tensor from experiment[9] .....	28
Figure 26:Variation of shear strain at mentioned points.....	29
Figure 27: Hybrid III dummy and impactor initial position. ....	31



Figure 28: Rotational (a) displacement and (b) acceleration profiles at CG of head during frontal impact.....	31
Figure 29: Linear (a) displacement and (b) acceleration at the CG of head. ....	32
Figure 30: Variation of linear acceleration with velocity at the CG of head [22]. ....	32
Figure 31: Hybrid III dummy with helmet and impactor initial position .....	33
Figure 32: Helmeted dummy impact profiles. ....	34
Figure 33: Boundary conditions for 2 dimensional model. ....	35
Figure 34: Integration points for shear strain measurement. ....	36
Figure 35: Shear stress variation at maximum stress zone in case of with and without helmet at points (a) 1, (b) 2, (c) 3 and (d) 4 as mentioned in above figure. ....	37
Figure 36: Pressure variation with linear and rotational displacement profile inputs. ....	38
Figure 37: Pressure variation inside brain at the time of impact in case of linear displacement (pressure in Pa). ....	38
Figure 38: Pressure variation in case of with helmet. ....	39
Figure 39: Max. principal stress variation in frontal part of brain. ....	39
Figure 40: GHBMC model no helmet front impact. ....	40
Figure 41: GHBMC model front impact with helmet. ....	41
Figure 42: Linear acceleration comparison of with and without helmet. ....	42
Figure 43: Rotational acceleration profiles (a) no helmet (b) with helmet during GBBMC model impact simulation. ....	42
Figure 44: Comparison of angular acceleration with and without a bike helmet [31]. ....	43
Figure 45: Impact forces on skull with and without helmet. ....	43

## LIST OF TABLES

---

Table 1: Human head material properties .....	18
Table 2 : Material properties of Isotropic ACH helmet shell. ....	20
Table 3: Material properties of Low Density Foam Pads .....	21
Table 4: GHBMC M50-P v. 1.5 Model General Information .....	23
Table 5: Contact definitions for helmeted GHBMC model.....	41



## **INTRODUCTION**

The human brain is very complex and extensive research is aimed at understanding its behaviour and function. Many scientific inquiries are published to clearly understand the functions that result from the interaction of about 86 billion neurons with 100 trillion connections. Though there is overwhelming interest and major research initiatives are focused on how our brain operates but still comparatively little is known about brain functions at the mechanical level.

Understanding of head loading occurring in motor vehicle crashes is a subject of ongoing research. This loading can be of two types contact or non-contact type which produces complex brain response sometimes with very high severity. Computational models are now extensively used in analysis of head impact in motor vehicle crashes. Finite element models are now anatomically very detailed and can represent complex response of brain very accurately.

### **1.1 Traumatic Brain Injury**

Traumatic brain injury (TBI) is a major health concern, conservative estimates indicate that nearly 1.6 million people suffer from TBI annually in India. Road traffic accidents and falls are identified as the leading causes of TBI among the Indian population. Knowledge of brain deformations during accelerative or impact loading is critical for the overall management of TBI, including the development of injury thresholds and personal protective equipment.

Among various injuries on the battlefield in US, traumatic brain injury (TBI) has become a common injury among the soldiers. A recent RAND (Research And Development) report estimates that 3,20,000 service members or 20% of the deployed force (of total deployed 1.6 million) are potentially suffering from TBI. In addition, researchers found that about 19 % of returning service members report that they might have had TBI during deployment, with 7 % reporting both a brain injury and major depression [1]

The TBI has a wide range of symptoms. Some effects are obvious immediately after the injury, whereas some may appear days, weeks or even years later. Loss of consciousness, nausea, dizziness, mental depression, blurred vision, and headache are some of the acute TBI symptoms. Hence, it is critical to understand the mechanics of TBI to formulate the mitigation strategies and to reduce the cost involved in treating it. To understand the mechanics of TBI different models are developed.

## **1.2 Mechanisms of Traumatic Brain Injury**

Broadly brain injuries are classified in two categories: focal injuries and diffuse injuries. The focal brain injury is responsible for local damage which can be seen through bare eyes. The diffuse brain injury is responsible for global disruption of brain tissue usually and remains invisible. The focal injuries are epidural hematomas (EDH), subdural hematomas (SDH), intracerebral hematomas (ICH), and contusions (coup and contrecoup). The diffuse injuries consist of brain swelling, diffuse axonal injury (DAI) and concussion.[2] The primary cause for these injuries is rotational or linear acceleration. Based on the type of acceleration classification of these injuries is given below.

### **1.2.1 Brain Injuries Induced by Rotational kinematics**

#### **Concussion**

The cerebral concussion is the most common type of head injury which involves the immediate loss of consciousness after injury. Among the injured 95% of patients can recover within one month and 99% of the patients left the hospital in 14 days [3].

#### **Diffuse axonal injury (DAI)**

Diffuse axonal injury is related with mechanical disruption of many axon due to shear strain in cerebral hemisphere and subcortical white matter (fig. 1). Through the microscopic examination of brain we can see the axonal tearing throughout the white matter of hemispheres. High resolution CT scans can show small amount of hemorrhages and axonal swelling (fig. 1) There is immediate loss of consciousness after DAI which can last for days to weeks. Severe memory loss, is present and posttraumatic amnesia can last for many weeks. After one month, 55 % of the patients are likely to lead to death [4].

## Contusions

After the head injury cerebral contusion is the most frequently found lesion. It involves pulping, heterogeneous area of necrosis, hemorrhage and edema [5]. During impact if the head is suddenly decelerates than there is relative motion between brain and skull. Brain continues to travel inside the skull and damage occurs during impact with skull. This results in 'coup contusion'. Contusions at the opposite side of impact are known as 'contrecoup' injury (fig. 1). A threshold value of 0.19 principal logarithmic strain in cortex leads to 50% risk of contusions induced by vacuum [6].

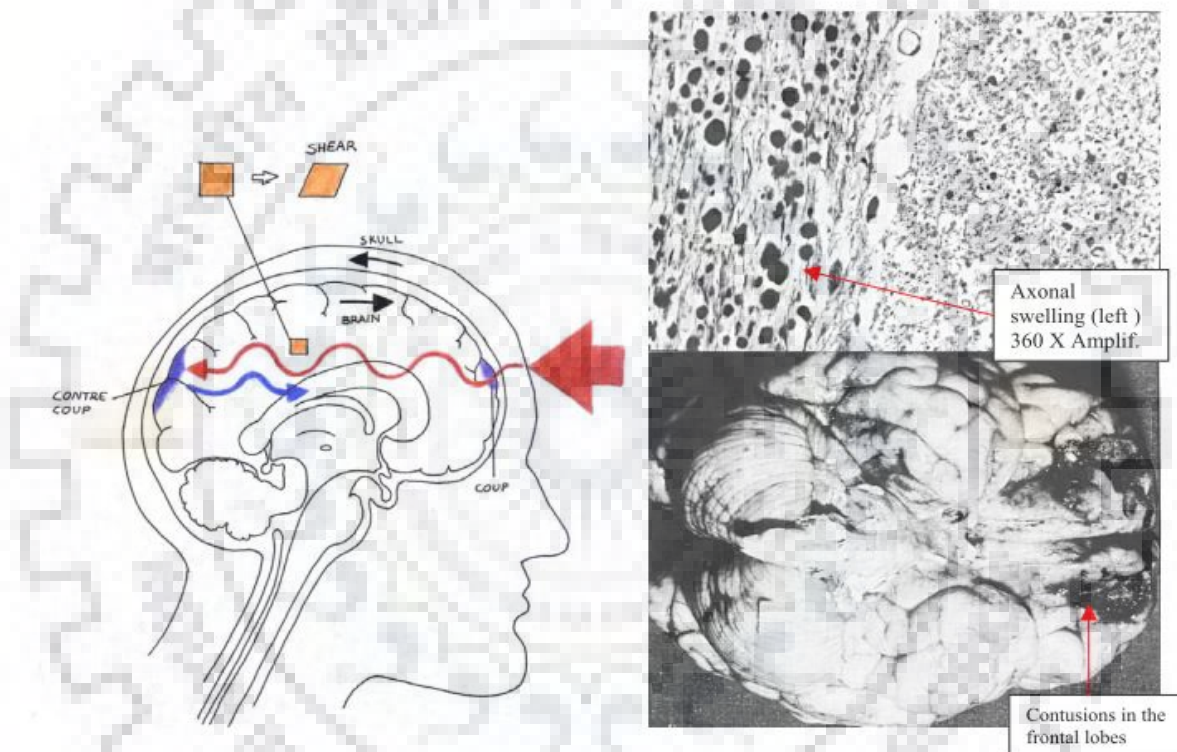


Figure 1: Biomechanics of DAI and Contusions

## Subdural hematoma (SDH)

Shearing of brain from inside of the dura is the most common cause of a subdural hematoma. This causes tearing of bridging veins that goes from brain surface to various sinuses (fig.2). In this case the mortality rate found in most studies is greater than 30%.

## Intracerebral hematomas (ICH)

Homogeneous collections of blood found in cerebral parenchyma are known as Intra-cerebral hematomas (ICH). Studies has indicated that the risk of ICH can be predicated by magnitude and

pattern of maximum principal strain. Other causes of this type of injury are blows and penetrating wounds to the head.

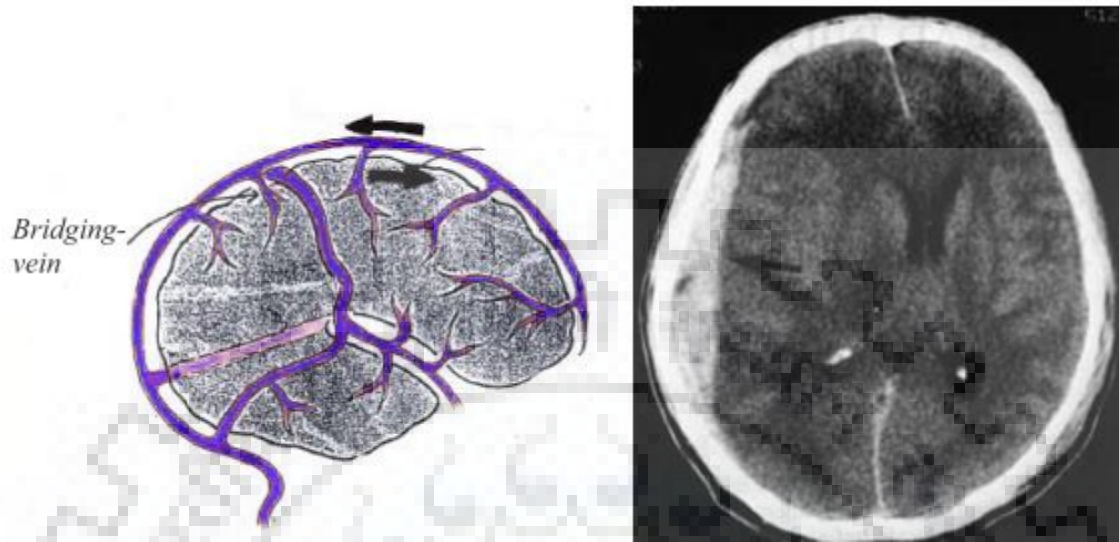


Figure 2: Subdural hematoma

### 1.2.2 Brain Injuries Induced by Linear kinematics

#### Skull Fracture

When there is direct impact on head higher contact forces and large linear accelerations are produced that increases the stresses on the skull bone. The stresses predict the risk of skull fracture (fig.1). The skull fracture forces vary according to impactor surface area. The value of these forces can be related to linear acceleration of head by Newton's law of motion. In a study it is estimated that a peak acceleration of 180g (gravities) can induce 5% risk of skull fracture and 250g can leads to 40% risk of fracture [7].

#### Epidural Hematoma (EDH)

It is result of the skull and underlying meningeal vessels trauma. EDH do not occur due to brain injury[5].

### 1.3 OBJECTIVE OF CURRENT WORK

Recent investigations suggest that rotational acceleration induced due to rotation of the head is more deleterious than the linear acceleration in causing TBI. Current helmets are neither designed nor tested for rotational loading. During this research, we propose to study

mechanics of head rotation under impact loading conditions. We specifically define following two objectives

- (i) To study the brain biomechanics under rotational loading.
- (ii) To study the effectiveness of the helmets and different types of foam pads in mitigating head acceleration.

We have studied rotational loading and foam effectiveness in our simulations on simple 2 dimensional models with brain material properties close to actual human brain and very detailed model of GHBMC.



This chapter deals with the past studies conducted for understanding the intracranial loading mechanics due to blunt impacts. The key findings in those studies along with the limitation of the studies are also presented. Since numerous studies have been carried out for blunt impact loadings and the related head loading mechanisms. Various studies on different test subjects have been carried out to unravel the actual mechanics of blunt induce TBI. Commonly used test subjects are in vitro cell culture, in vivo animal models, mechanical head models, cadaver head models, and numerical models. These subjects are selected based on the mode of injury and the severity of TBI studied. For instance, in vitro model represents the cellular level injury model followed by an animal model that represents the tissue level injury model. Finite element methods are extensively used in figuring out the details loading process that are not possible in the experiments.

## **2.1 Finite Element Studies Review**

In experimental method the entire process preparations of head, preservation the integrity of brain tissue by using perfusion system and implanting of sensors to head is very laborious. Variabilities comes from the preparation of samples and several experimental factors which leads to causes variations in results & interpreting of results becomes more difficult. Hence often finite element model is being used to study the TBI in human model. Although in finite element model the variations in results is small due to unknown material properties of each component in model. Whatever finite element model provides clear understanding of TBI.

The FE models are also used for to determine the role of personal protective equipment (helmet) [8]. FE model, head form and actual cadaver head are the appropriate models to check the role of PPE and improve the design to mitigate TBI. To check the performance of helmets, test subjects are fitted with helmets and are subjected to different types of loading.

Lee et al. (1987) used a 2D finite element model of the head of a rhesus monkey to better understand the role of head acceleration in subdural hematoma. He studied the combined effects of tangential and angular acceleration on bridging vein deformation and compared the simulation results with experimental data. He concluded that angular acceleration is more deleterious than



translational acceleration in tearing of bridging veins. The brain was modeled with isotropic homogeneous elastic material and skull was treated as a rigid material. The tied constraint was used between interfaces. To measure the deformation of bridging brain change in distance between a node at brain and a node at skull was observed [9].

Chu et al. used 2D finite element model and observed that pressure and shear stress magnitude in a sagittal plane are independent of direction of motion [10].

Gilchrist et al. used 2D plain strain finite element model incorporating all the major parts of head. In midsagittal plane, they investigated the dynamic response of human head under direct impact load conditions. They modeled the brain as a viscoelastic material instead of elastic material to correctly see the effect of brain stiffness. The coup and contrecoup pressure were measured in both the cases i.e. elastic and viscoelastic brain (fig.3). They concluded that the viscoelastic brain can represent the brain in a more realistic way [11].

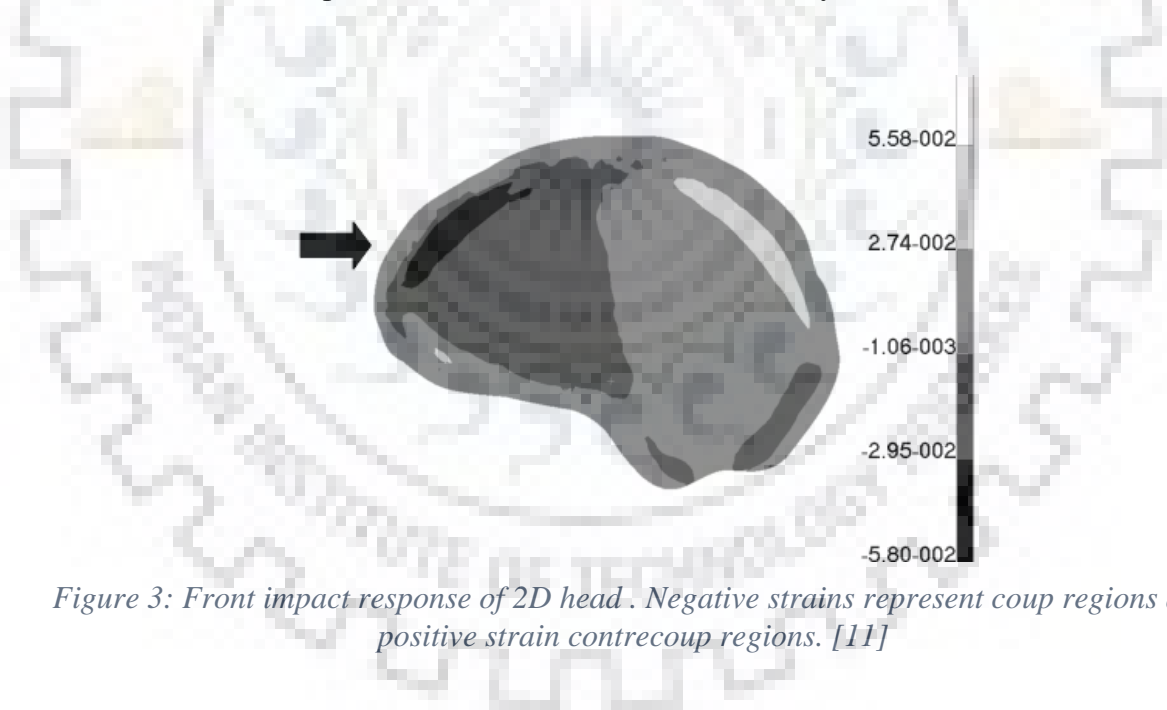


*Figure 3: Front impact response of 2D head . Negative strains represent coup regions and positive strain contrecoup regions. [11]*

Ueno and Melvin (1995) did impact simulation study on Hybrid III dummy and obtained the profiles of acceleration. They applied these profiles on 2D model of head. They concluded that if we apply linear and rotational profiles separately than it predicted the lower severity compared the actual injury. Also, they told in their results that due linear acceleration coup and contrecoup injuries (which are pressure induced) arises rotational acceleration is responsible for shear deformation in the brain [12].

Zhou et al. (1995) simulated the impact response of parasagittal bridging veins using one dimensional string elements and predicted higher risk of injury at the central part of sagittal sinus because during rebound it could be subjected to higher tensile strains. He applied acceleration pulse on the model and showed that strain are higher during deceleration than acceleration in bridging veins. He concluded that the direction of impact in case of subdural hematomas [13].

Zhang et al. (2001) used a 3D FE model to study the differences between frontal and lateral brain responses. They applied tied boundary condition between the skull and brain which restricted the relative motion between them. They concluded that in case of lateral impact there is more shear stress and more positive pressure (fig.4) in core areas of the brain. So there are more chances of diffuse axonal injury due to increased shear stresses in the brain [14].

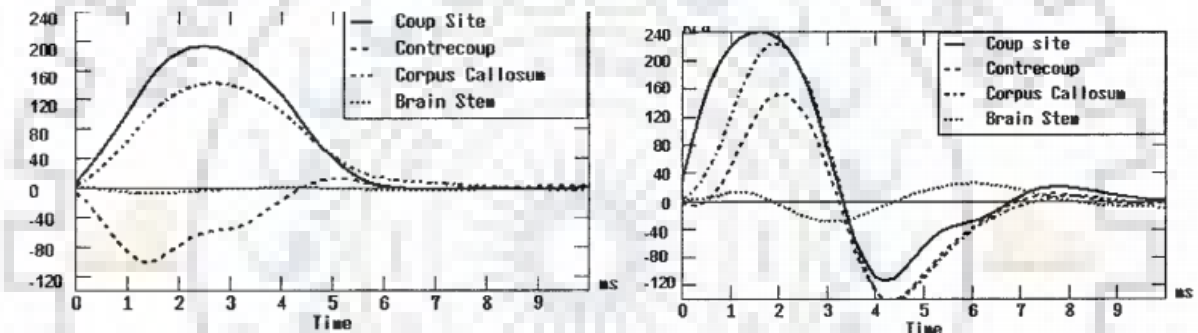


Figure 4 : (a) Frontal impact (b) lateral intracranial pressure responses [14]

## 2.2 Experimental Studies Review

Test subjects that are robust and consistent in performing TBI studies are mechanical models. Mechanical head models are sometimes called as headforms. The major limitation of the mechanical model is their lack of biofidelic characteristics. Hence, they are less popular when compared to other test subjects. Mechanical test subjects are simple to build, could be instrumented easily, and could be varied in different sizes and shapes.

Mechanical head models are available in various forms and sizes. In mechanical models, each parameter in the study like materials involved, positioning of the subject with respect to loading, size and shape of the model, location of sensors and other variables are clearly known. Hence, results drawn from the mechanical models are concrete and thus understanding the basics behind the loading mechanics can be made clearer and stronger.

Mechanics of stress wave propagation in the skull and its effect on the brain, pressure propagation in the brain, deformation of the head and other basic phenomena occurring during the loading can be studied thoroughly using mechanical subjects. The conclusions drawn from the mechanical models are useful for animal and human model studies. Distinct experiments can be designed on the animal and cadaver models based on the conclusions from the mechanical models.

Holbourn (1943) experimented on a parasagittal section of the brain made of gelatin and noted the shear strain pattern inside the brain. He concluded that linear acceleration produce compression and rarefaction strains which do not cause any major injury. There is no relative motion between skull and brain in case of linear acceleration. Major cause of brain injury is shear strain which are produced due to rotation because brain has nearly incompressible material properties [15].

Unterharnscheidt (1971) did impact studies on cat head at various speeds and explained that repeated impacts of low velocity can produce injury in the brain. He applied the rotational acceleration of different magnitude on squirrel monkeys and found lower magnitude caused subarachnoid hemorrhages. Monkeys subjected higher magnitude rotational acceleration were not survived [16].

Gennarelli et al. (1972) studied the controlled sagittal plane head motions of 25 squirrel monkeys. No cerebral concussion was obtained in 12 out of 25 monkeys which were subjected to peak linear acceleration of 665-1230g. Remaining 13 monkeys which were subjected to rotational acceleration producing tangential acceleration of 348-1025g found concussed [17].

Hodgson et al. (1979) took a freshly dead Macca monkey's brain hemisection model and subject it to pure linear, pure rotational and combined motions. They measured brain-skull relative displacement and shear strain at various locations. They found that the shear strain produced due to pure rotation was highest and long lasting. In their experiment the highest shear strain was measured in brain stem instead of periphery of brain [18].

Hardy et al. (2001) used a high speed biplanar x-ray system and neural density targets (NDTs) to measure relative displacement between brain and skull. They used human cadaver heads to study 3D relative displacement patterns and found it was in the range of -5mm to +5 mm [19].

Hardy et al. (2007) used the same technique of biplane x-ray and NDTs (fig.5) to measure intracranial pressure, relative displacement and maximum principal and shear strain. They showed variation of these parameters with the use of helmet. With higher linear acceleration peak maximum principal strain and maximum shear decreased, peak coup pressure increased. With the use of helmet translational and angular acceleration reduced but corresponding strain increased [20].

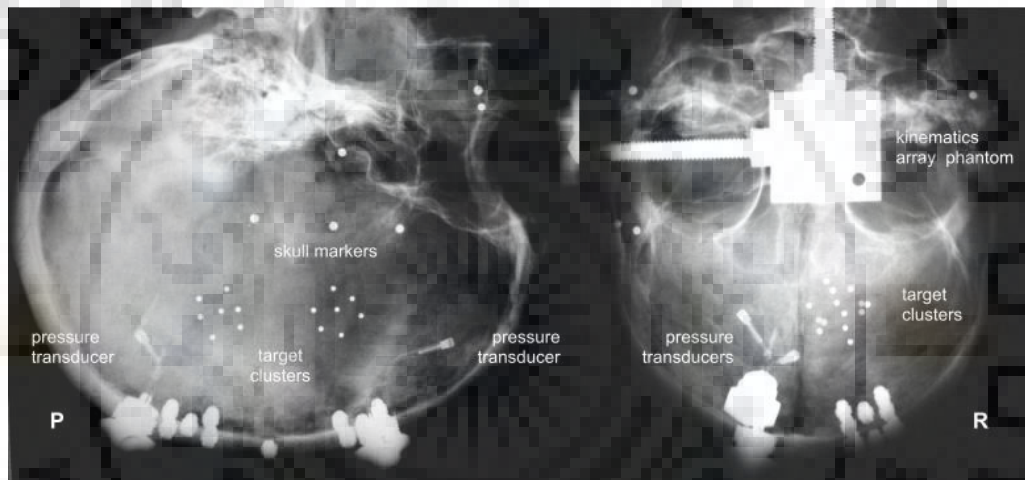


*Figure 5: Representative instrumentation x-rays showing the NDT clusters [20]*

P.V. Bayly et al. (2007) used a new measurement technique, magnetic resonance imaging (MRI) to see the transient response of a cylinder filled with gel which is subjected to angular acceleration. Displacement and strain were measured with high spatial and temporal resolution with this technique. These strain fields were compared with a mathematical closed form solution and FE simulation of shear waves using the same boundary and initial conditions. During the experiments he found shear strain values within 10% (.01 strain), the same result was predicted with finite element simulations of the cylinder. This technique can be used for measurement of shear wave inside brain when angular acceleration applied on skull [21].

Ievgen Levadnyi et al. (2017) studied traumatic brain injury during impact in various configuration i.e. frontal, temporal, parietal etc. at different velocities ranging from 1 to 7 m/s. They also studied impact injuries in case of with and without helmet using different parameters

i.e. HIC, foam pad thickness, shell thickness etc. They concluded that helmet protect injury by reducing HIC. The foam thickness is the most critical parameter during design of helmet. With the increase in foam thickness HIC decreases, while increase in helmet shell thickness increases effective HIC [22].

Post et al. (2011) examined ice hockey helmets for impact induced injury and found that peak linear and angular acceleration were not the good parameter for prediction of brain injury. A lower magnitude of linear acceleration have the risk of brain injury which can pass through standard certifications of safety. Deformation of the brain is the best criteria for assessing brain injury [23].

### **2.3 Summary**

Though many studies have been carried out to understand the mechanics of TBI, there are no comprehensive and concrete conclusions for angular acceleration induced diffuse axonal injury in case of the helmet. Hence, a simple comprehensive study is required to clearly identify the parameters of helmet related injury i.e. mass, inertia, foam properties, thickness, etc. The computational models of human are more reliable when compared to the models of animal and cadaver. So we have used a simple 2D model having all the major parts of the human head and detailed full body human model for better understanding of mechanics behind brain injury.

### 3.1 Introduction

In this chapter we have described the 2 dimensional human model development, ACH helmet and foam pad finite element model preparation, material properties of brain, skull, csf, helmet and foam. Different solution scheme during analysis are also described. In our study we have used 3 types of models – (a) 2 dimensional plain strain model (b) Hybrid III human dummy and (c) Global Human Body Models Consortium (GHBMC) full body detailed model. With 2D model and hybrid III dummy we have done combined study to understand the effect of rotational and linear acceleration. Later we have simulated head impact on GHBMC full body model. All models are presented in detail in this chapter.

### 3.2 2-Dimensional Finite Element Model Description

To perform numerical analysis and obtain reliable results, we need to check that behaviour of our FEM model and real human head is similar. The magnetic resonance imaging (MRI) now a days used widely for diagnostics and construction of FEM 3D and 2D models which are used in simulation studies of various biomechanical studies.

A two-dimensional plane strain finite element model was constructed in the mid-sagittal plane of the head using the image obtained from MRI scan of a human head as shown in figure (6.a) and (6.b).

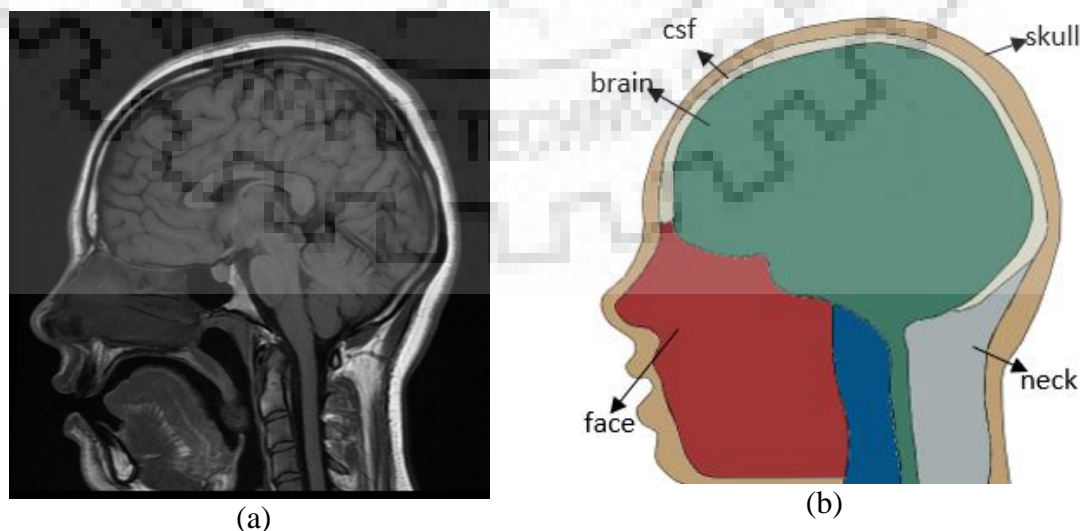


*Figure 6: (a)MRI scan of a human head in the mid-sagittal plane (b) 2D CAD model made in Solidworks.*

All major parts of human head i.e. brain, csf, face, neck, skull were modeled using single layer finite elements. The length of the model measures 170 mm from anterior to posterior and, as such, represents an average male human head. Total number of nodes in the model 9912 and total number of elements in the model 9225.

Reference point (rp-1 and rp-2) were taken as shown in figure 7 to apply different boundary conditions. Rp-1 is located on neck mid point and Rp-2 is located on the centre of area of the model.

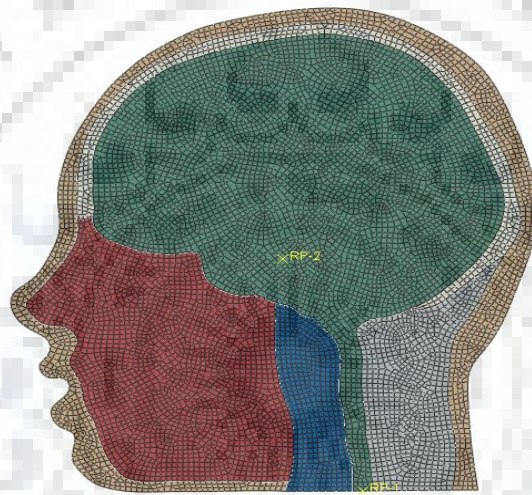


Figure 7: FEM model with mesh and reference points.

Tie constraint was applied among all the parts instances (i.e. brain and csf, csf and skull etc.). Rp-1 was constrained as kinematic coupled with outer surface of the skull to perform Bayly's experiment [21] on the model. The model was validated with the Bayly's results.

### 3.3 Materials Models

The next stage of the modeling was to add material properties for different structures of the head. The material property of the brain tissue is assumed to according to Rashid et. al. (2014) properties [24].

#### 3.3.1 Viscoelastic Material Model

Viscoelastic materials exhibit both viscous and elastic characteristics when undergoing deformation. This results in time-dependent behavior, which means that a material's response to deformation or force may change over time.

Viscoelastic materials respond differently depending on how fast they are stretched. Displacement is related to strain so strain rate is defined as how fast a material is stretched. So viscoelastic materials are said to be strain rate dependent (fig-8).

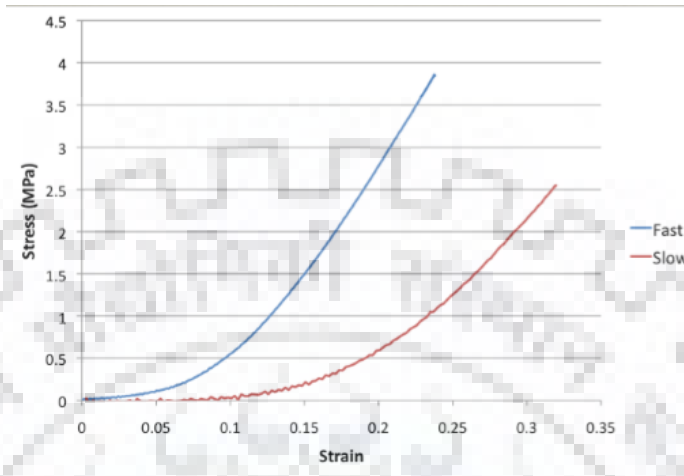


Figure 8: Stress-strain diagram for viscoelastic material at two different strain rates.

If we apply a constant displacement to a viscoelastic material, then the force to hold the material in this position decreases over time it is known as stress relaxation (fig-9).

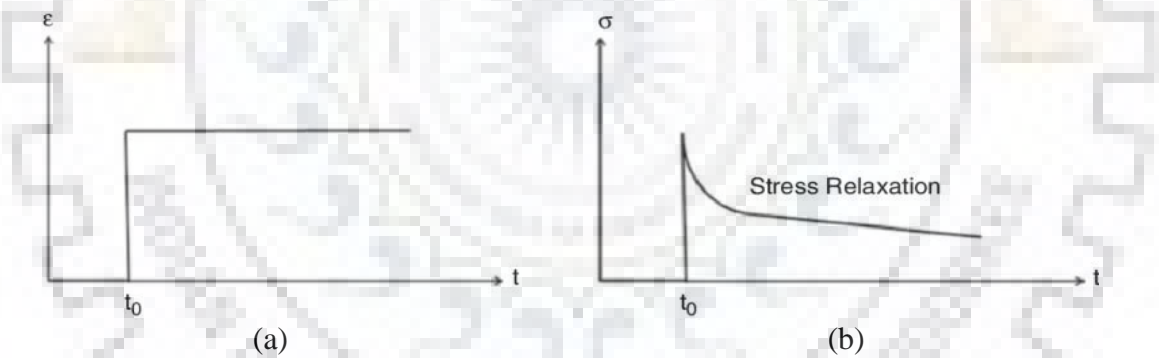


Figure 9: Stress relaxation behaviour of viscoelastic material (a) initial applied strain (b) stress.

If we apply a constant force to a viscoelastic material, then the displacement increases over time. When this force is released, it takes time for the material to recover to its initial position (fig-10). It is known as creep in viscoelastic material.

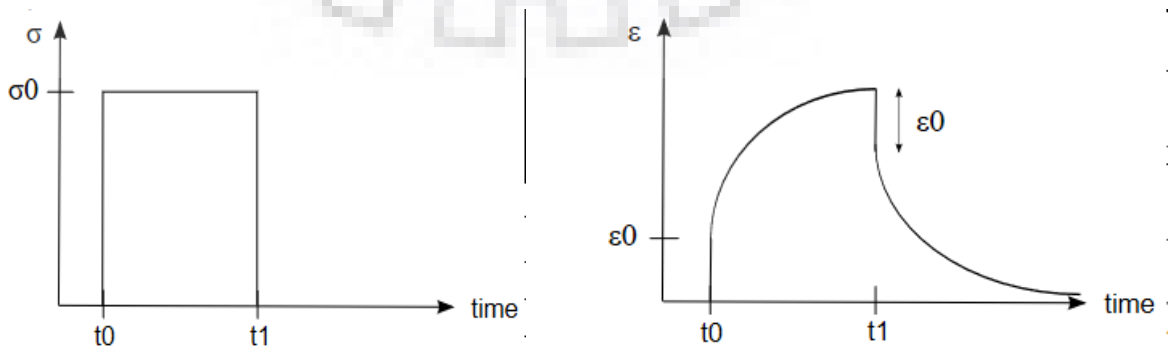


Figure 10: Creep in viscoelastic material (a) applied stress (b) corresponding strain with time



When viscoelastic materials have a force applied to them and then removed, it takes more energy to displace the material than it does to return the material to its original position. So it consumes more energy in loading phase than unloading phase. This energy difference is caused by the material losing energy during the loading phase, due to heat dissipation or molecular rearrangement within the material. This is known as hysteresis of viscoelastic material.

**Viscoelastic material properties of brain:**

Viscoelasticity is expressed in an N-term Prony series as:

$$\mu(t) = \mu(0) \times [1 - \sum_{i=1}^n g_i ((1 - e^{-\frac{t}{\tau_i}}))] \dots\dots\dots (3.1)$$

Where,  $\mu(t)$  – Shear modulus at time t.

$\mu(0)$  – Initial shear modulus.

$g_i, \tau_i$  – Material constants

We used a two term Prony series,

$$\mu(t) = \mu(0)[1 - g_1 (1 - e^{-\frac{t}{\tau_1}}) - g_2 (1 - e^{-\frac{t}{\tau_2}})] \dots\dots\dots (3.2)$$

The constants of the equation are:

$$g_1 = 0.5663, g_2 = 0.3246, \tau_1 = 0.035, \tau_2 = 0.0351, \mu(0) = 2780 \text{ Pa}, \mu(\infty) = 303.3 \text{ Pa}$$

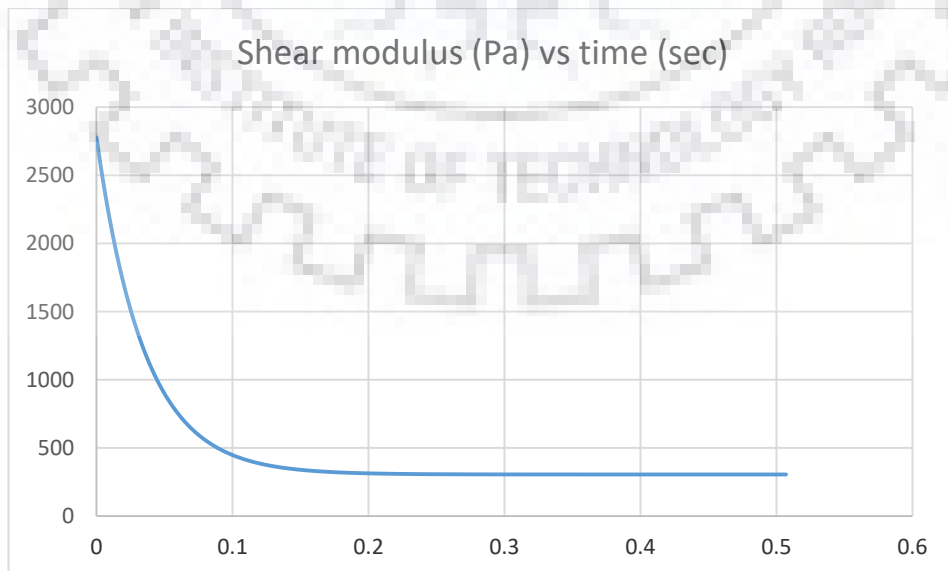


Figure 11: Shear relaxation curve

After plotting equation (3.1) in excel, we get the shear relaxation curve as shown in Figure 11. Then we entered all these parameters in Abaqus viscoelastic material program under prony series model.

### 3.3.2 Hyperelastic Material Model

Hyper elastic materials have non-linear relationship between stress and strain. The stress-strain relationship also depends on the rate of stress application (fig-12). It is used in large deformation problems for foam, rubber etc. like materials.

Hyperelastic materials use strain energy density function to derive stress-strain relationship. When strain is even between 100% to 700% this allows them to accurately model the relationship between stress and strain.

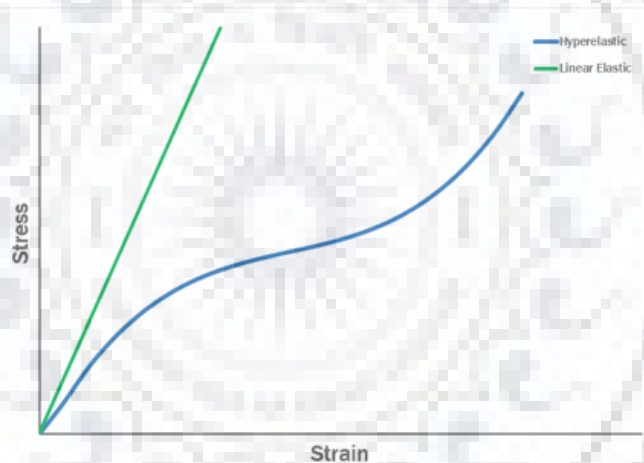


Figure 12: Stress-strain curve for linear elastic and hyperelastic material.

#### Hyperelastic material properties of brain:

An Ogden form hyperelastic model with N-terms has the following strain energy function,

$$U = \sum_{i=1}^n \left[ \frac{2\mu_i}{\alpha_i^2} (\lambda_1^{\alpha_i^2} + \lambda_2^{\alpha_i^2} + \lambda_3^{\alpha_i^2} - 3) \right] + \sum_{k=1}^N \frac{(J-1)^{2k}}{d_k} \dots\dots\dots (3.3)$$

$$U = \sum_{i=1}^n \left[ \frac{2\mu_i}{\alpha_i^2} (\lambda_1^{\alpha_i^2} + \lambda_2^{\alpha_i^2} + \lambda_3^{\alpha_i^2} - 3) \right]$$

Where,

U – Strain energy function

$\mu_i$  ,  $\alpha_i$  ,  $d_k$  – Material constants

$\lambda_1, \lambda_2, \lambda_3$  – Deviatoric principle stretches

J - determinant of the elastic deformation gradient

We are using first order strain energy potential function.

$$U = \frac{2\mu_1}{\alpha_1^2} (\lambda_1^{\alpha_1^2} + \lambda_2^{\alpha_1^2} + \lambda_3^{\alpha_1^2} - 3)] + \frac{(J-1)^2}{d_1} \dots\dots\dots (3.4)$$

Material parameters used in model,

$$\alpha_1 = 6, \mu_1 = 926.66, d_1 = 14.4851$$

Calculations of the parameters:

$$d_1 = \frac{2}{K_0}$$

$$K_0 = \frac{2}{3} \times \mu_0 \times \frac{(1 + \nu)}{(1 - 2\nu)}$$

Where,  $K_0$  – Initial bulk modulus

$\mu_0$  - Initial shear modulus

$\nu$  – Poisson's ratio

We know,  $\mu_0 = 2780 \text{ Pa}$

$$\nu = 0.49$$

Thus,  $K_0 = 138.073 \text{ MPa}$

$$d_1 = 14.4851$$

$$\mu_0 = \frac{1}{2} \sum_{i=1}^N \alpha_i \mu_i$$

$$\text{Thus, } \mu_1 = 2 \times \frac{\mu_0}{\alpha_1} = 926.66$$

We modeled the brain-skull interface using cerebra-spinal fluid (CSF) approach. The brain bathes in CSF. It maintains a uniform pressure inside cranium in normal head and performs an important function to protect the brain from jolts that would cause it to hit the bony walls of cranium. We used CSF average thickness of approximately 4mm. Different materials used for different parts are shown in given table (1).

**Table 1: Human head material properties**

Component	Young's Modulus (MPa)	Poisson's ratio	Density (kg/m <sup>3</sup> )
Brain	-	0.49	1040
Skull	8000	0.22	2070
Face	15000	0.22	2000
Neck	1000	0.24	1300
CSF	9.85	0.49	1133

### 3.4 3-D Helmet and Foam Model

Helmet is used as personal protective equipment (PPE). It is used to damp the forces that arises during the impact on head hence it provide safety to the brain and skull. We took a surface mesh of Advanced Combat Helmet (ACH) model and imported it in Hyper mesh. Helmet shell was created by extruding the surface mesh inward up to a distance of 10 mm with 8 noded solid elements. Two layers of elements were used throughout the thickness. 5786 elements were used with average element size 6 to 8 mm (fig-13.a).

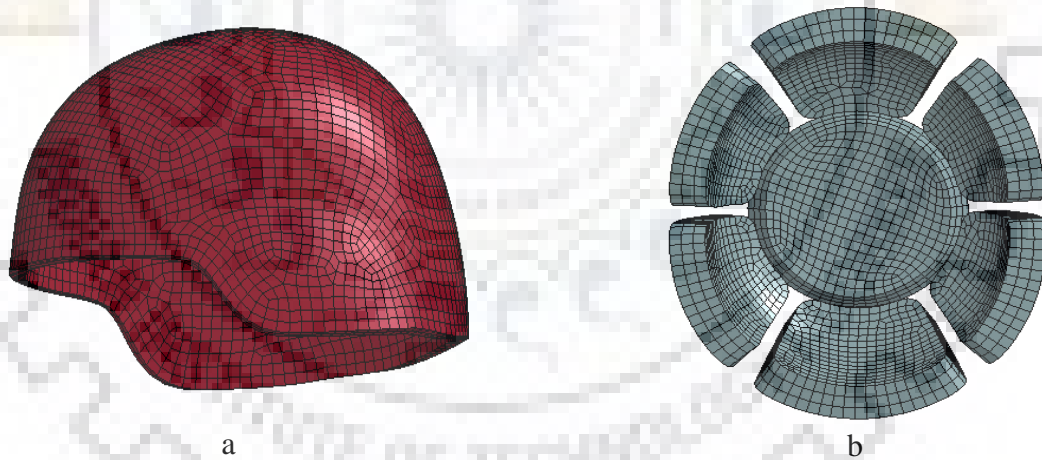


*Figure 13: ACH helmet (a) shell (b) foam pad.*

ACH helmet has another component which is seven pad suspension system (fig-13.b).. To model the foam pad first surface were created and then extruded inward throughout the pad thickness which is 19 mm. Three layers of 8 node brick element were used through the thickness having average mesh size of 5 mm to 6 mm. 4665 elements were used in the model. We exported these models in LS dyna for our simulations. A combined model of real ACH helmet and FE ACH model in shown in fig-14.

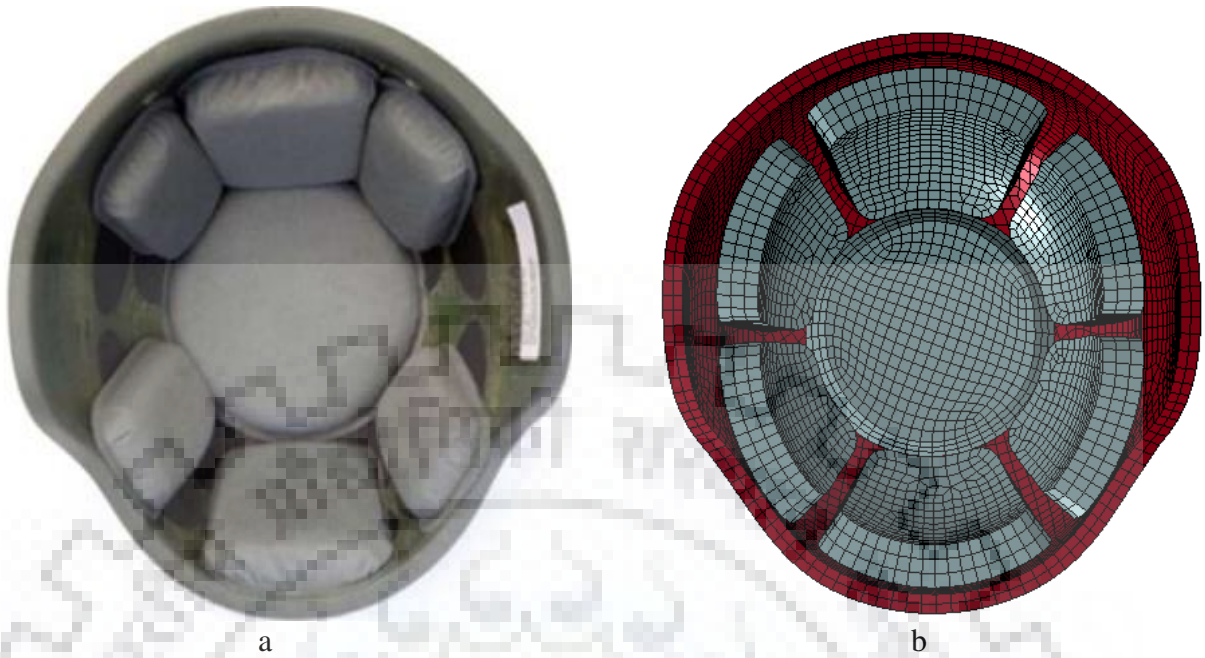


Figure 14:(a) ACH helmet with pad (b) FE model of ACH helmet.

Foam material will absorb energy when the helmet shell impacted with some force. Foam can deform when low relative stress is applied on it. It can reduce peak acceleration by reducing peak force applied on helmet. A indicative stress-strain curve for foam material is shown in figure-15 it shows the compression of foam.

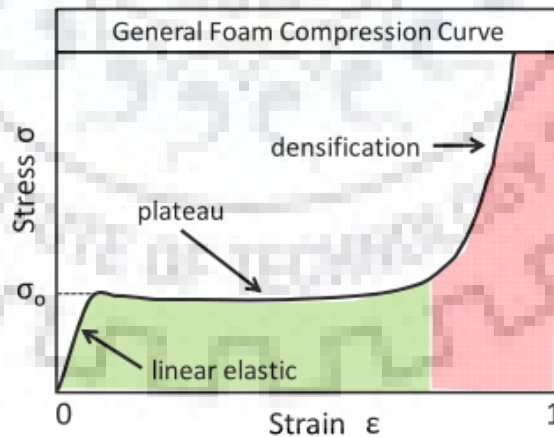


Figure 15: Indicative stress-strain curve for foam material [25].

There are three distinct regions in general stress-strain diagram as shown in figure: (1) Linear elastic (2) plateau and (3) densification. When foam is compressed in plateau region during impact it can absorb energy and safeguard the head reducing the chances of serious brain injury. We

should insure that foam thickness must be sufficient during compression in plateau region so it do not reach in densification region.

Energy is dissipated during loading and unloading cycles of foam material which is measure of hysteresis losses. This energy is absorbed due to internal structure. The rebound energy divided by total absorbed energy is known as hysteresis unloading ratio. The foam material which immediately rebounds from its compressed state could have negative impact on protection. Theoretical hysteresis curve is shown in figure 16.

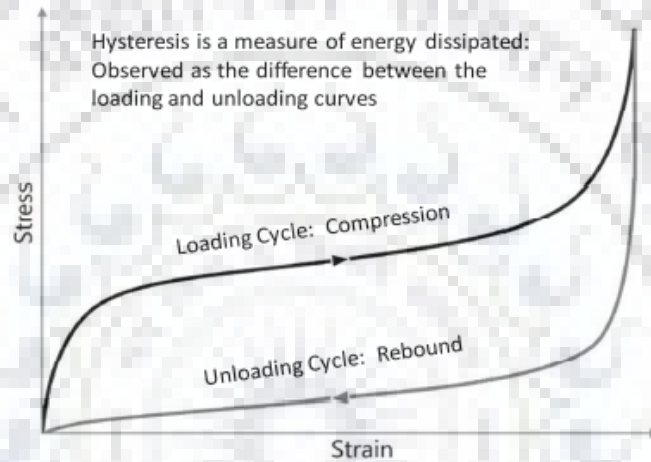


Figure 16: Hysteresis curve for foam material [26]

The material model for the outer shell of helmet is MAT\_012 ISOTROPIC ELASTIC PLASTIC in LS DYNA (LSTC, Livermore, CA, USA). The material parameters are taken from literature [27] as mentioned in table 2.

Table 2 : Material properties of Isotropic ACH helmet shell.

Ro (kg/mm <sup>3</sup> )	G (GPa)	SIGY (GPa)	ETAN	BULK (GPa)
1.230e-006	7.400000	0.0770000	0	12.330000

The ACH helmet pad material parameters are chosen as provided by manufacturer Team Wendy. Pad has polyurethane based foam material properties. The MAT\_LOW\_DENSITY\_FOAM (MAT\_057) is selected in LS-DYNA which can properly represent the foam behaviour i.e. all the three stages of compressible foam (i.e., linear elastic, plateau, and densification). The stress-strain behaviour of this material is dependent on loading rate. We have used hard foam material properties in our simulations which is valid in case of impact because it absorbs the impact energy. This material model requires different parameter i.e. uniaxial stress-strain curve, elastic modulus,

density, shape factor, hysteresis unloading factor, damping factor etc. which are given in table-3 and taken from literature [27].

**Table 3: Material properties of Low Density Foam Pads**

Ro (kg/mm <sup>3</sup> )	E (GPa)	TC (GPa)	HU	DAMP	SHAPE
6.300e-008	0.0084000	10	0.25	0.10	5.0

Uniaxial compression curve are provided by manufacturer at different strain rates 0.02, 0.2, 2, 20, and 200 s<sup>-1</sup> at a normal strain of 80% base on compression tests conducted. We have used the stress-strain curve obtained at 200 s<sup>-1</sup> at normal strain of 80% which is shown in figure 17.

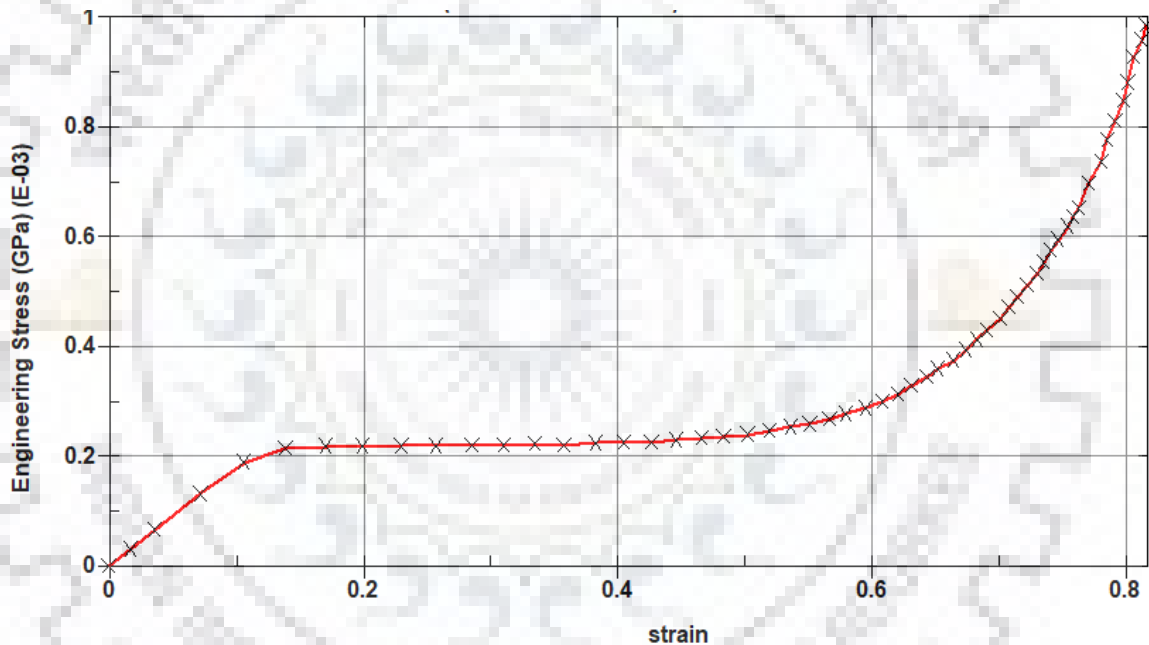


*Figure 17: Uniaxial stress-strain curve for hard foam [28].*

### 3.5 Hybrid III Human Dummy Model

Hybrid III dummies are widely used test devices in injury assessment and crash testing, also known as Anthropometric test devices (ATDs). In the physical model of these dummies different types of materials are used i.e. rubber, foam, steel, vinyl, aluminum etc. to maintain proper bio fidelity and measure injury severity. We have used Finite Element model of Hybrid III dummy model (LSTC.H3\_50TH\_FAST.120702\_V2.0) in our simulations. FE models of these dummies are extensively validated for head and neck acceleration, chest deflection, chest acceleration etc. So results obtained from these dummies are reliable to assess to crash severity and human safety.

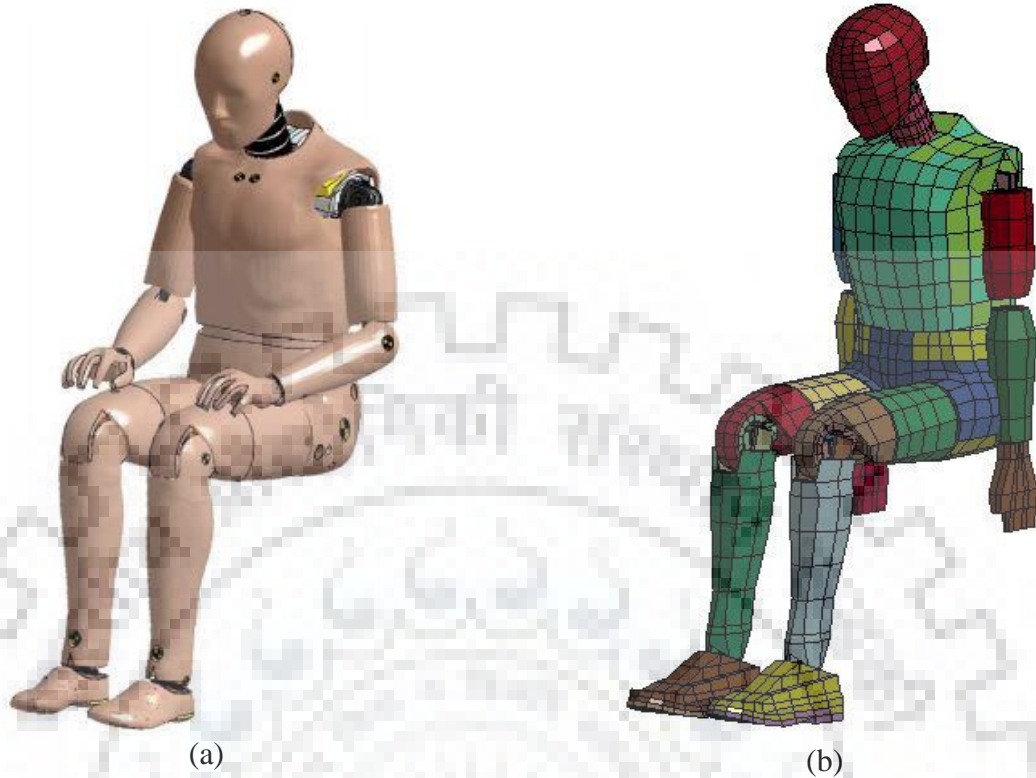


Figure 18: (a) Hybrid III 50th Percentile Crash Test Dummy (b) Fast FE model of 50<sup>th</sup> Hybrid III dummy [29]

We have used this dummy to completely capture the neck response during impact analysis. Because we wanted to know how the rotational and linear acceleration changes with rotation of neck. Fast model of dummy is used instead of detailed model because only kinematics of head acceleration and displacement is required, also it reduces the simulation time. Neck assembly is modeled with four rubber discs, 5 metal discs, neck to head connection bracket, steel cable for tension at the center, bracket on upper neck to mount on spine (figure-19).

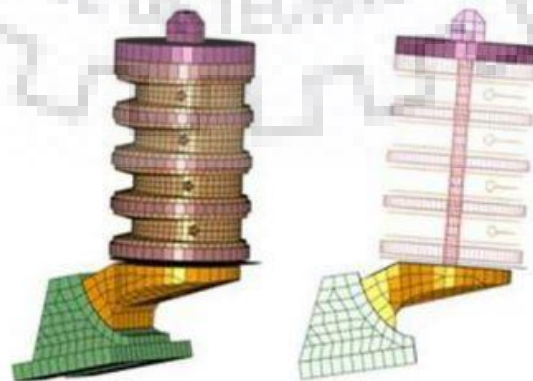


Figure 19: FE model of neck for Hybrid III dummy [29]



In this dummy neck rubber components are modeled as three dimensional solid elements and discs have different depth to capture neck motion. Tied node to surface contact is used between rubber and metal discs. Steel cable is modeled as beam elements and metal disc as 3 dimensional fully integrated solid elements. These steel cables are under tension initially for this “initial stress beam” option is used in the model. These models can capture neck motions (i.e. flexion and extension) as specified in standard of Federal regulations (figure -20). Overall kinematics of neck is very close to physical model.

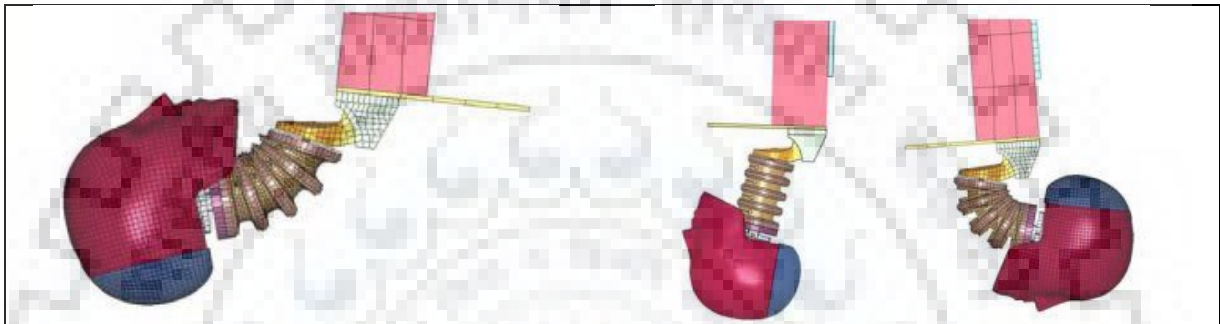


Figure 20: Maximum flexion and extension of FE neck head assembly [29]

### 3.6 GHBMC Full Body Model

Biofidelity and stiffness of anthropometric test devices (ATD) or dummies is different from real life human body, as these are designed to capture kinematics of human body. In order to obtain reliable data these models should be validated with PHMS test data. So to capture the real life response of frontal impact test on human we have used the Global Human Body Model Consortium (GHBMC) full body detailed model (figure-21). This model represents 50<sup>th</sup> percentile standing male with detailed anatomical geometry. The model has extensively validated against various literature studies for different biofidelity aspects i.e. different loading condition, rate of impact etc. General information about the model are given below in the table-4.

Table 4: GHBMC M50-P v. 1.5 Model General Information

<b>Model version:</b>	GHBMC M50-P v. 1.5
<b>Elements (millions):</b>	2.32
<b>Nodes (millions):</b>	1.25
<b>Number of Parts:</b>	1,005
<b>Mass (kg):</b>	77.5

We have used LS Dyna R.10.0 with ls-dyna\_mpp\_s\_R10.0\_winx64\_ifort131\_msmpi solvers. We mounted our helmet model on the head of this GHBMC model and simulated the frontal impact test. The simulation time for 25 milliseconds run is almost 4 hour with 32 mpp cores on our workstation.

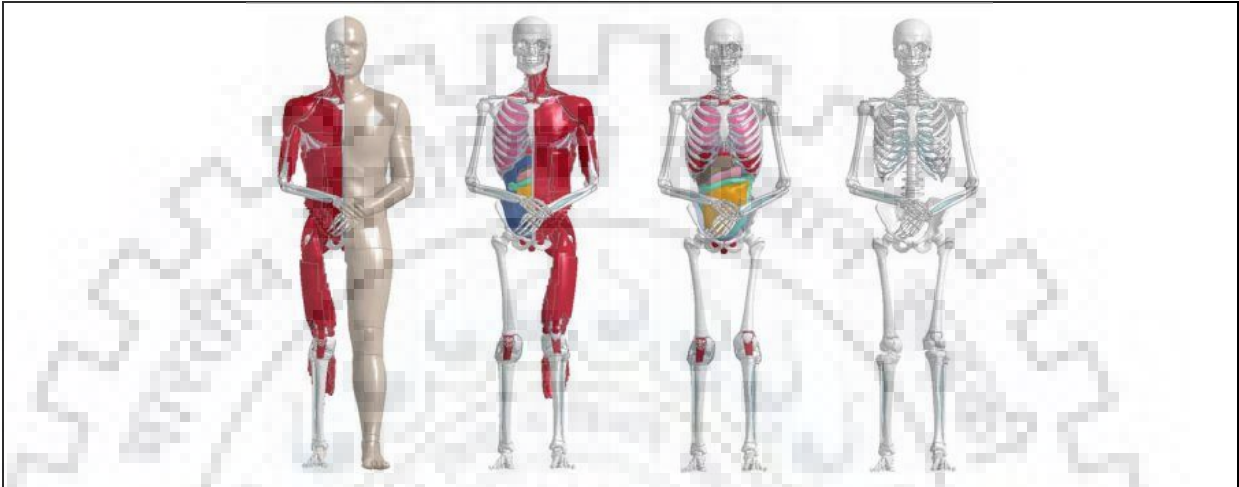


*Figure 21: GHBMC M50 detailed Pedestrian full body model [30]*

### **3.7 Solution Scheme in Abaqus**

The finite element model is solved using nonlinear transient dynamic procedure. In this procedure the governing partial differentiation equations for conservation of momentum, mass and energy along with material constitutive equation and equations defining the initial and the boundary conditions are solved simultaneously. We have used explicit/dynamics type solution scheme in Abaqus® 2016, since our problem is dynamic type problem. In explicit scheme velocity, acceleration and damping is considered, hence solution becomes a function of time. It uses central difference methods and accounts propagation of sound speed. Step size has been selected such that it should not be greater than transit time for each element either heavy mesh distortion can takes place. For each time step, it makes new mass matrix & calculates the displacement at every time increment. Explicit method uses central differences time method for nonlinear ordinary differential equation hence it is used for nonlinear problems. We have run the simulation for simplified two dimensional cylinder head model subjected to different profiles of linear and angular displace or acceleration.

In this work automatic time stepping is used with explicit central –difference time integration. In automatic time stepping time increment for each increment is calculated based on the minimum element size and wave speed. Time increment is calculated based on given equation.

$$t_{inc} = \sqrt{\frac{L_{min}}{c}}$$

Where  $L_{min}$  minimum element is size and  $C$  is wave speed.

### 3.8 Solution Scheme in Ls Dyna

We have used latest version of Ls Dyna R.10.0 with MPP solver. Our simulation problem contains analysis of large deformation response of foam pad assembly, dynamics response of impact on deformable and rigid body structures, so we have used nonlinear explicit three dimensional FE code. Lagrangian formulation with central difference method is used to solve equations of motion for a continuum in time. Ls Dyna uses various types of contact algorithms, which are well suited for contacts like hard to soft material surface contact, shell element contact, single surface contact etc. It also permits gap, offset, constraint, sliding, manual contact stiffness etc. in contact formulation.

### 3.9 Summary

In this chapter we have described the 2-d model, Hybrid III dummy model, helmet and foam model, GHBMC full body model in detail. These models are used with the described properties to analyze the response of impact induced linear acceleration, angular acceleration, stress, strain etc. in case of with and without helmet. Brain material properties, which is critical parameter in study of traumatic brain injury, are described. Approach to solve the finite element code is also described in this chapter. The results obtained using these models are described in next chapter.

### 4.1 Introduction

How does the human brain deform during rapid angular acceleration of the skull, to see this phenomenon we replicated Bayly's experiment on our model. Simulations were performed in two dimensions under the assumption that all deformation occurs in the plane of rotation (plane strain). The transient response was simulated for a time interval of 0.07s.

### 4.2 Load

The impact can be assumed as sinusoidal pulse. So we applied a sinusoidal pulse of  $250 \text{ rad/s}^2$  for 40 ms as shown in figure 4.1

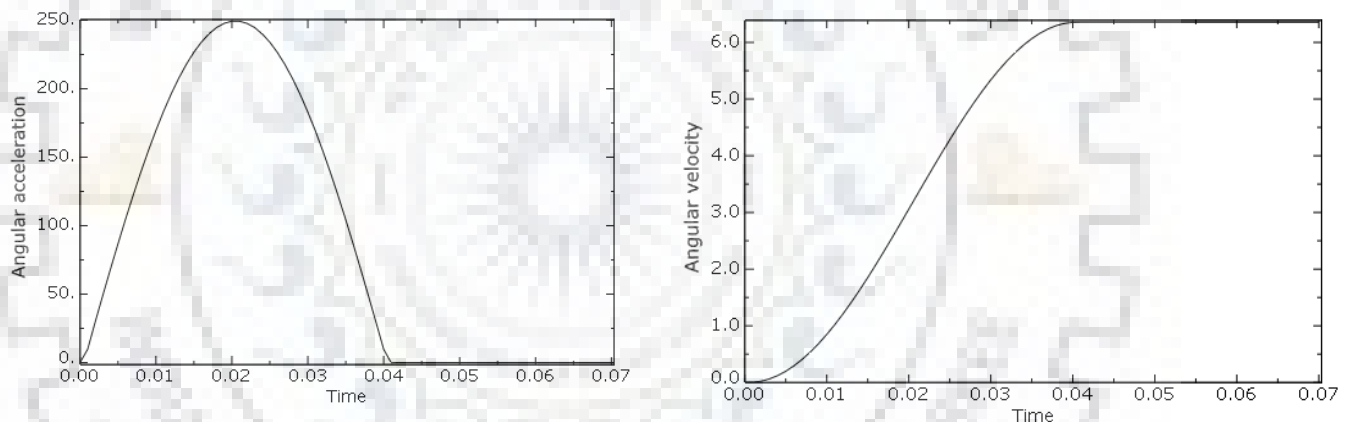


Figure 22: Profile of applied acceleration pulse and corresponding velocity

### 4.3 Boundary Condition

We took a reference point on the neck of the model and applied kinematic coupled constraint at this point with outer surface of the skull as given in figure. At reference point we applied the given acceleration sinusoidal pulse with magnitude  $250 \text{ rad/s}^2$ .

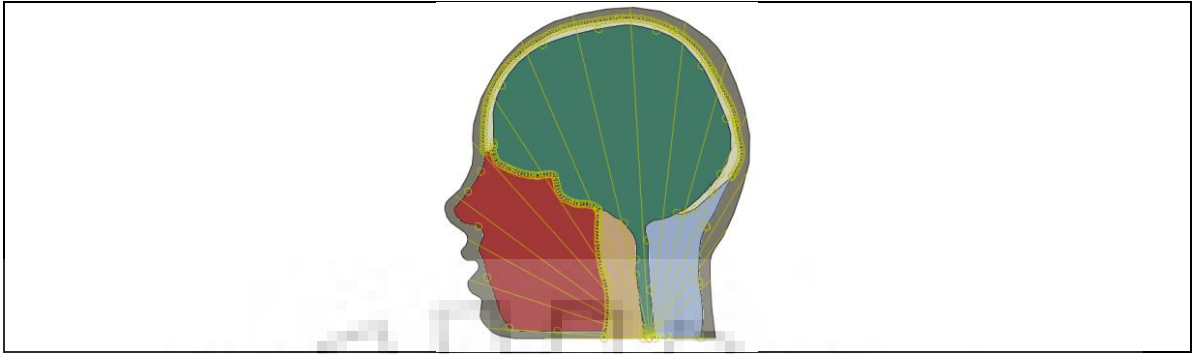
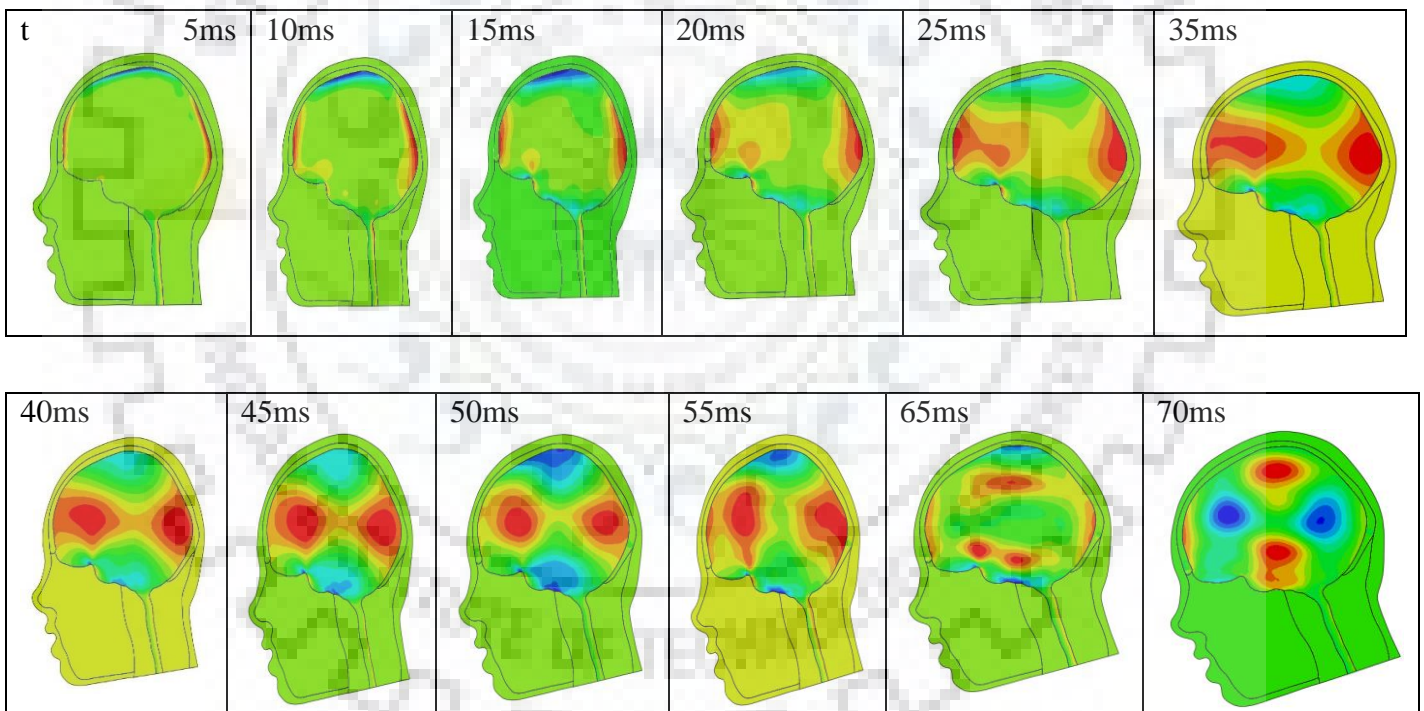


Figure 23:Reference point and constraint

#### 4.4 Simulation Results

We measured the shear strains inside the brain and observed the shear strain within the range of (-.1 to +.1) as observed in the Bayly's results [9]. We came to know how the propagation of shear wave takes place in the brain. Coup and countercoup regions can be seen like shown in figure 24



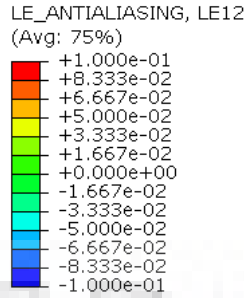


Figure 24: Variation of shear strain inside the brain

According to Bayly's Measurements of the 2-D Lagrangian strain tensor were obtained with 4 mm spatial resolution and 6 ms temporal resolution during propagation of transient shear waves in a cylindrical sample of a viscoelastic gel. The strain field was dominated by radial circumferential shear, as expected for waves excited by angular acceleration of the cylinder boundary. Close qualitative and quantitative agreement was obtained between experimental measurements, analytical solutions, and predictions of a 2-D FE model. Throughout the entire spatial domain and temporal duration, experimentally measured shear strain values were within 10% (0.01 strain) of those predicted by FE simulation [9]. In this experiment the strain variation inside the given head are shown in figure 25.

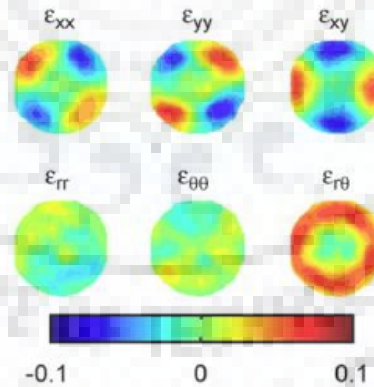


Figure 25: Components of the Lagrangian strain tensor from experiment[9]

So we measured the shear strain in different coup and countercoup regions (where shear strain is maximum or minimum) and the results were found within the limit as shown in figure 26

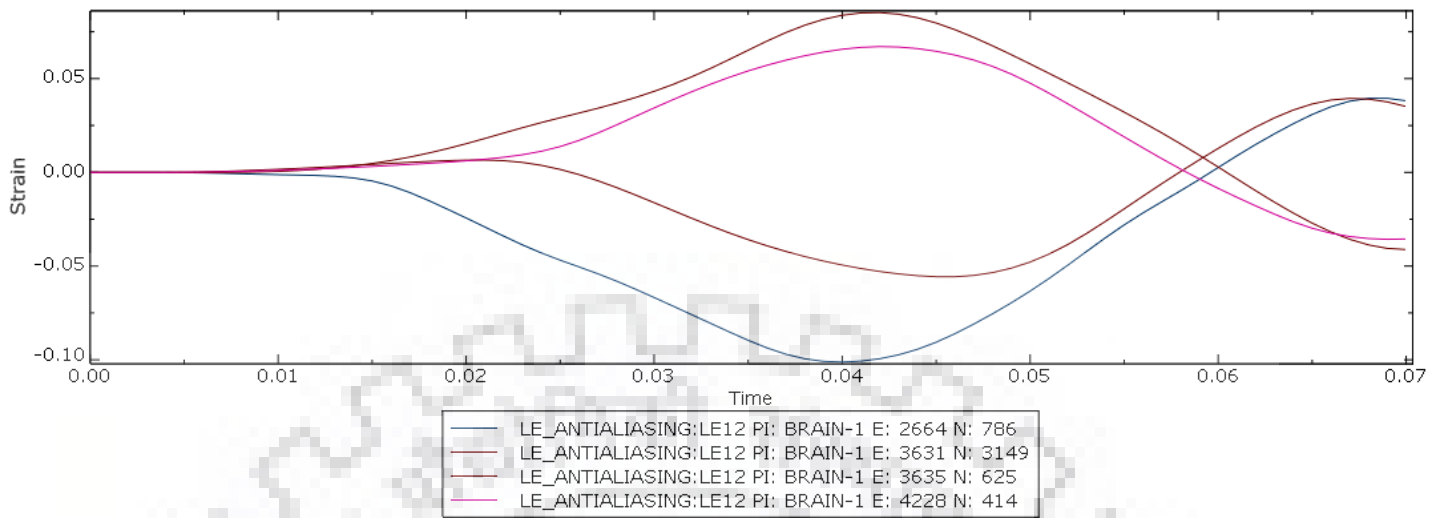


Figure 26: Variation of shear strain at mentioned points

### **5.1 Introduction**

In literature we have found that linear acceleration has given more importance over rotational acceleration in assessment of brain injury. The famous Head Injury Criteria (HIC) is also based on linear acceleration which is used in many standards of TBI. Traditionally both the accelerations have been studied independently. But both of these accelerations contribute in brain injury as suggested in many studies. It is found that linear acceleration is related to intracranial pressure [20] while rotational acceleration is responsible for shear strain deformation of brain [3].

In this chapter we have discussed the role of helmet in mitigation of head injury and compared linear acceleration, angular acceleration, shear strain, pressure etc. injury criteria in case of with and without helmet. Hybrid III and 2D head model are used to combined study of helmet because dummy provides only kinematic details, no information about stress strain in the brain. So we extracted the acceleration and displacement profiles form dummy's center of gravity and applied to CG of 2D model. Later we used GHBM model for this study and compare the results.

Having validated the present two-dimensional finite element model by means of the Bayly's investigations under rotational condition, a series of progressively more sophisticated analyses was carried out to simulate the biomechanical response of the head to frontal impact conditions.

### **5.2 Hybrid-III dummy frontal impact**

To know the brain response in the frontal impact condition we performed our simulation in two cases (a) without helmet (b) with helmet. In two dimensional model exact neck response is difficult to model. So to capture the neck response and rotational acceleration of head we used Hybrid III dummy. Impactor has total mass of 16.5 kg which has properties of steel (modulus of elasticity  $E = 200$  GPa, poisson ration = 0.3). Initial velocity generation of velocity 3 m/s was given to impactor in Ls Dyna and SPC\_SET\_BIRTH\_DEATH option activated to stop it after 11 millisecond which prevented the problem of repeated impacts between head and impactor. Initially the impactor is kept 20 mm away from head and motion is allowed only in x- direction as shown in *Figure 27*. A boundary condition is applied to the back of dummy which restrict it's motion in y and z- directions. The simulation time is kept 400 milliseconds to capture the complete motion of neck and rotation displacement profile.





Figure 27: Hybrid III dummy and impactor initial position.

### 5.2.1 Simulation Results Without Helmet Impact

After application of given input condition, we tracked acceleration and displacement profiles at the center of gravity (CG) of head. The simulation time is almost 2 hours for 400 milliseconds runtime. We observed that maximum head rotation was almost 78 degrees (*Figure 28*). Maximum value of plane D rotation is 78.5 degrees as mentioned in Ls dyna dummy model manual. The neck completed more than one cycle during impact.

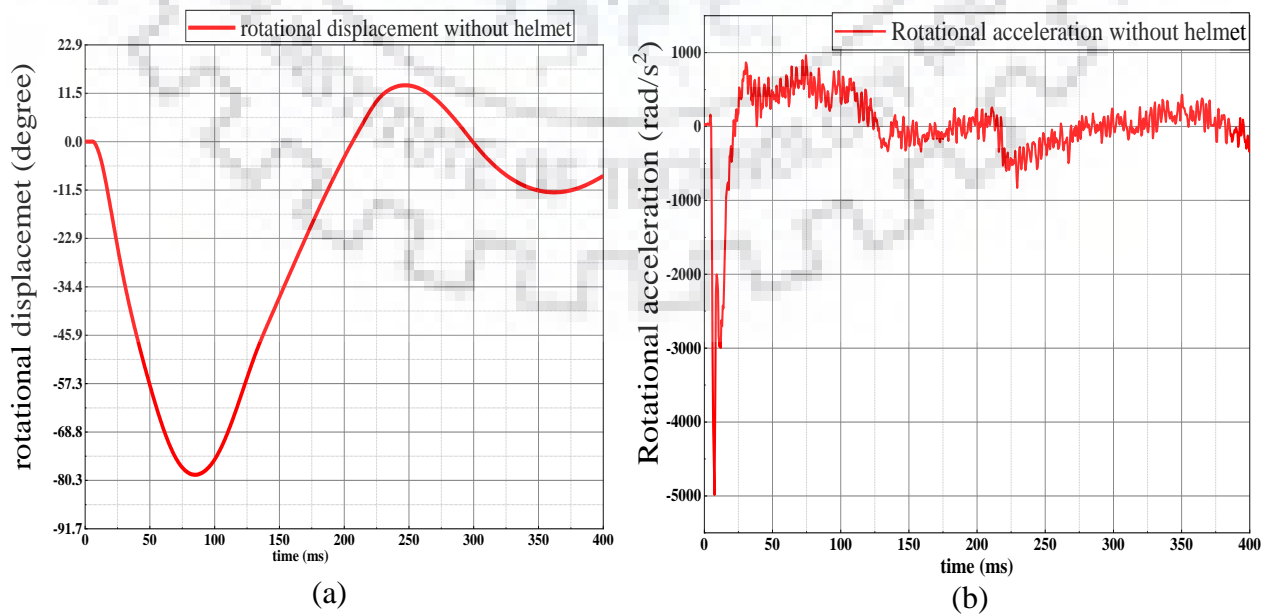


Figure 28: Rotational (a) displacement and (b) acceleration profiles at CG of head during frontal impact

We applied SAE 180 filter to extract the results of rotational acceleration as mentioned in dummy user guidelines. Linear acceleration profile of the CG of head is shown in *Figure 29*. Peak linear acceleration was 230 G ( $1G = 9.81 \text{ m/s}^2$ ).

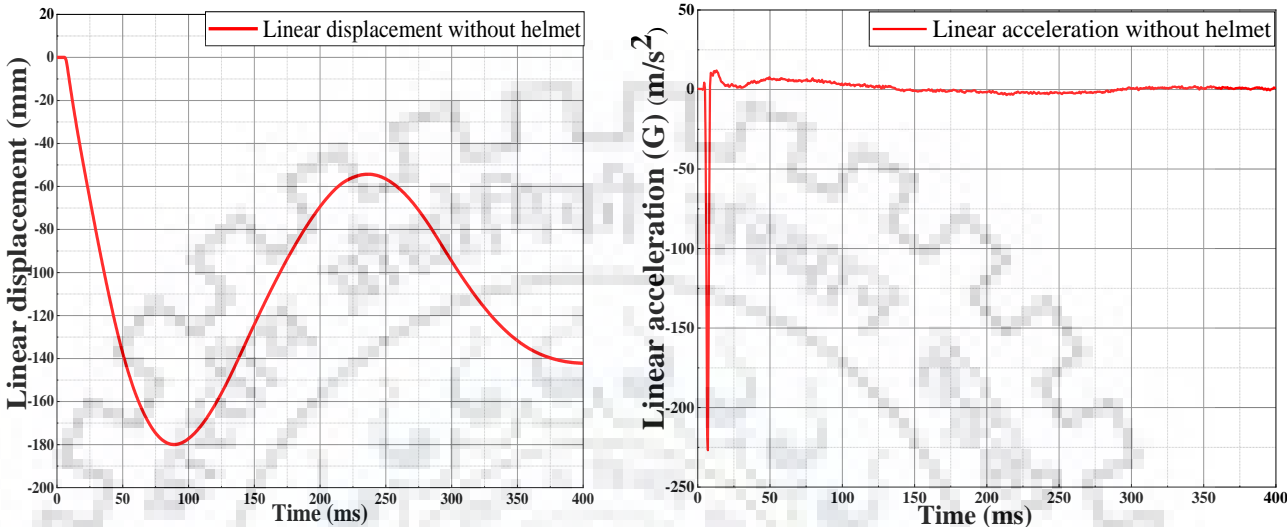


Figure 29: Linear (a) displacement and (b) acceleration at the CG of head.

Ievgen Levadnyi et al. [22] studied the effect of impact in different configurations i.e. frontal, occipital, temporal etc. and compared the results to find relationship with traumatic brain injury. They impacted the human model with velocities ranging from 1 to 7 m/s and presented the variation of linear acceleration and HIC with velocity (*Figure 30*). The frontal impact line is shown in blue color. There we can see corresponding to 3 m/s velocity head acceleration is  $240 \text{ m/s}^2$  which is comparable to our results obtained from dummy impact.

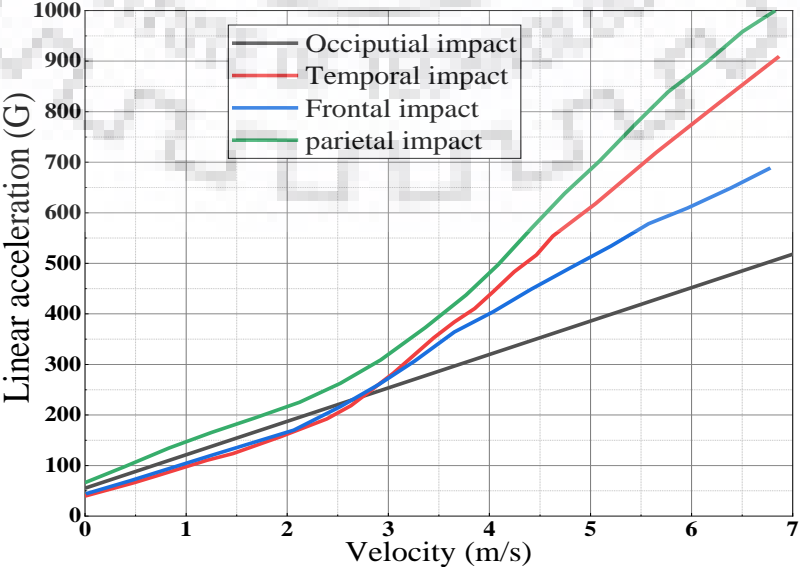


Figure 30: Variation of linear acceleration with velocity at the CG of head [22].

### 5.2.2 Simulation Results with Helmet Impact

We imported the helmet and dummy model in Hypermesh and positioned them such that helmet inner surface just touched the head surface. AUTOMATIC\_SURFACE\_TO\_SURFACE contact was applied between helmet and impactor. Helmet inner surface was tied with foam pad outer surface using TIED\_SURFACE\_TO\_SURFACE contact in Ls-dyna. Same contact is applied between foam and head. All other boundary and initial conditions were kept same as above to compare the results. The initial position with helmeted dummy is shown in *Figure 31*.



Figure 31: Hybrid III dummy with helmet and impactor initial position

In foam model we have used hard foam material properties because it absorbs impact energy. Tied contact between foam and head do not represent real life situations properly but it has simplified contact problem. A more realistic simulation has performed on GHBM model in which chin strap is used to hold the helmet in position. Various profiles extracted from CG of helmeted head are shown in *Figure 32*. Linear and rotation acceleration profiles are filtered at 180 Hz with SAE filter to see the significant results. We have the following observation by comparing with and without helmet impact cases.

(i) Maximum rotational displace in case of helmeted impact (36 degrees) is significantly less than without helmet impact (78 degrees) also the head completes more rotation in given time in helmeted case.

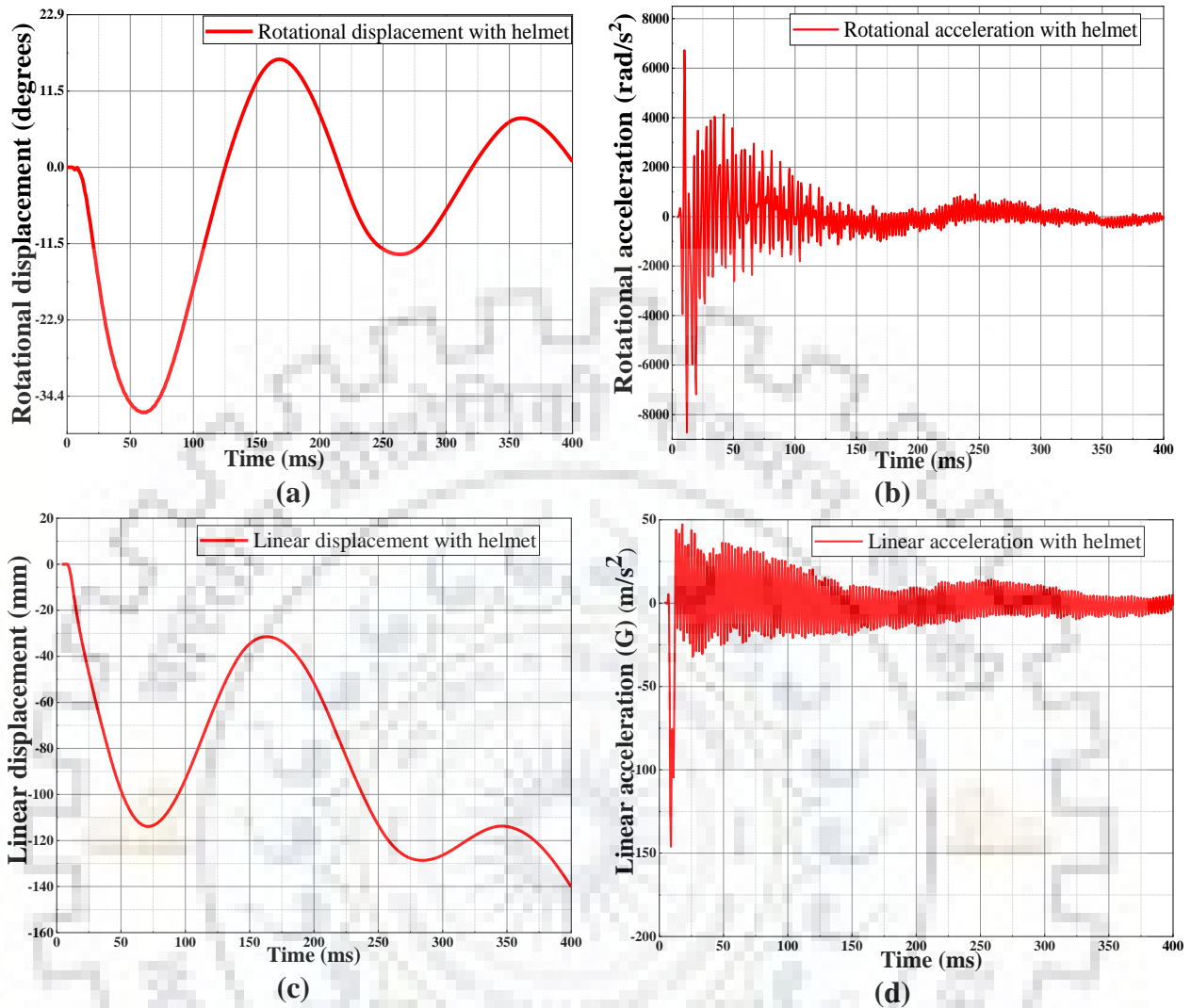


Figure 32: Helmeted dummy impact profiles.

(ii) Peak linear acceleration has reduced from 230 G to almost 150 G in helmeted head dummy. There are less chances pressure induced injury because almost 35 % reduction in peak linear acceleration.

(iii) Peak rotational acceleration has increased significantly in case of helmeted dummy which can induce more shear stress and strain, increasing the chances of diffuse axonal injury. There is large amount of fluctuations both linear and acceleration profiles, possibly due to tied contact between foam-head interface.

In these dummy model simulations, we can't see how the brain deforms locally. Hence we are unable to find local stress, strains, pressure etc. to access brain injury severity. So we used our simplified two dimensional plain strain model having all the major parts of human head.

### 5.3 Simulations On Two Dimensional Model

To see that how the human brain deform and what is the effect of shear wave propagation we applied these real life impact profiles of displacement and acceleration on 2 dimensional model. It is validated fact the helmet protects the brain under impact in linear acceleration conditions [22] but under angular acceleration condition it is a complex phenomenon and it has different results than linear acceleration.

#### 5.3.1 Boundary conditions

To study the helmeted and non helmeted head we applied kinematic coupling constraint on outer surface of the helmet and reference point on centroid of 2-d model. We selected the same surface area on the skull in no helmet condition and applied the same coupling constraint. We ran the simulation for 400 ms to capture the full rotation of the neck.

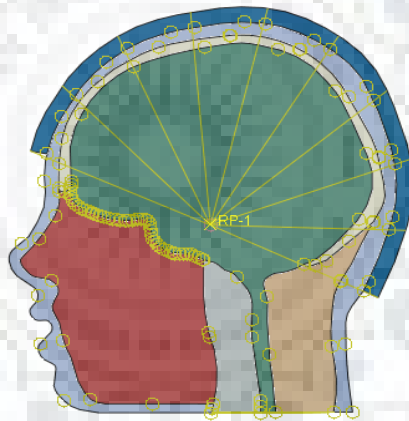


Figure 33: Boundary conditions for 2 dimensional model.

#### 5.3.2 Simulation Results

When we applied the acceleration and displacement profiles and measured these profiles in output signals, both profiles did not match due to a phenomenon called aliasing. Aliasing is a form of data corruption that occurs when a signal (i.e. acceleration) is sampled at a series of discrete points in time, but not enough data points are saved in order to correctly describe the signal. The aliasing phenomenon can be addressed using digital signal processing (DSP) methods, a fundamental principle of which is the Nyquist Sampling Theorem. So the sample should be sampled at a rate that is greater than twice the signal's highest frequency.

Aliasing depends on a number of factors i.e. output rate, output variables and model characteristics. The signals which have large amplitude oscillation at frequencies greater than half

sampling rate (the Nyquist frequency) may be distorted due to aliasing. So the safest way to avoid aliasing is to write the output at every stable time increment because it is based on the highest frequency response of the model. But it is not a practical way to resolve this problem as it results in a very large size output file (i.e. stable time increment in our model is  $10^{-7}$  seconds order). So to avoid aliasing we should request output at an appropriate rate with real time filtering to remove high frequency content from the results before writing the data to the output database file.

We have used an antialiasing filter in Abaqus for all our simulations to avoid aliasing which gives vague results if not taken care properly.

In both the cases with and without helmet we tracked the shear strain, maximum in plane principal stress and pressure variation profiles to compare both cases.

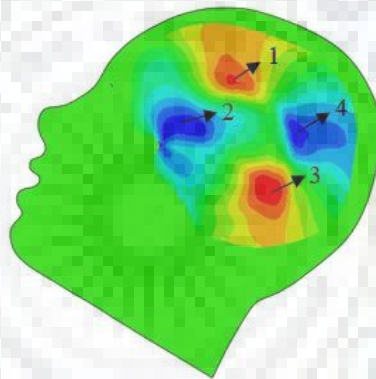


Figure 34: Integration points for shear strain measurement.

We applied the extracted profiles of rotational displacement in the corresponding model of with and without helmet. We measured the shear strain (LE\_12) in both cases at integration points (as shown in *Figure 34*) where maximum shear strain is expected. The shear strain variation with time at these points is shown in *Figure 30*. We observed interestingly that maximum shear strain after 0.05 seconds in case of helmet (35 %) was more than no helmet (15 %). The shear strain profiles at integration points 1 and 3 in case of positive strain, points 2 and 4 in case of negative strain are almost similar. We get a peak of shear strain just after the impact as the shear wave passes through given points. In case of helmeted head, higher shear strain is probably due to added mass and increased volume of helmet-head assembly.

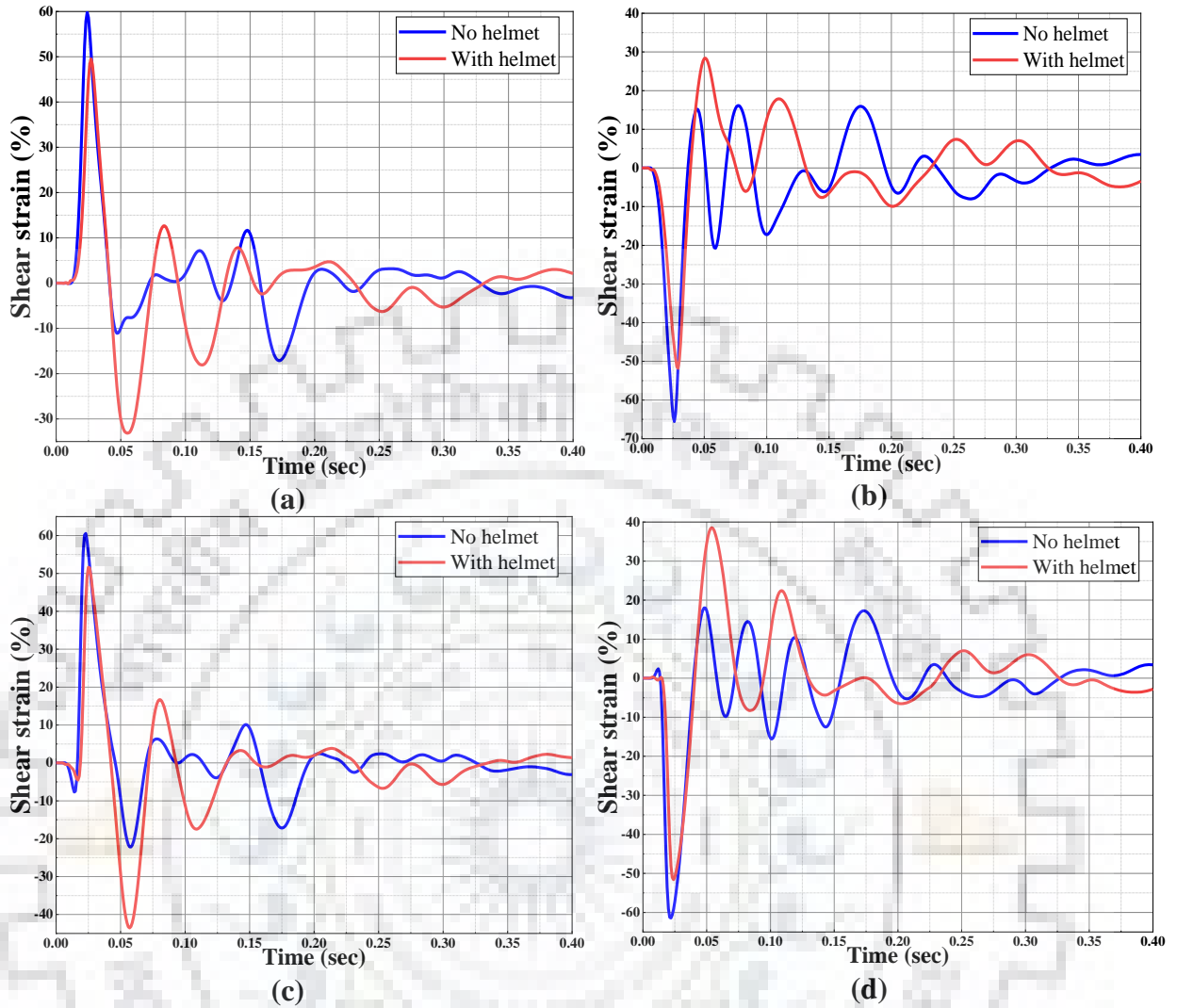


Figure 35: Shear stress variation at maximum stress zone in case of with and without helmet at points (a) 1, (b) 2, (c) 3 and (d) 4 as mentioned in above figure.

The brain is very sensitive and most important part of our head so to better understand the injury mechanics of impact we applied the linear and rotational displacement profiles about CG of head in without helmet case to study the pressure variation inside the brain (*Figure 36*). We got a peak pressure just after the impact on head. We can see in the figure that peak pressure (130 kPa) in case of linear displacement is very high as compared to rotational displacement input (peak pressure 18 kPa). Our peak pressure also matched with Ievgen Levadnyi et. al. [22] frontal impact case. So we can conclude that linear acceleration plays a major role in peak pressure and pressure induced injury, angular acceleration is less important in this case. When angular acceleration or deceleration increases suddenly than coup and countercoup brain injuries takes place due to immediate rise or fall of pressure.

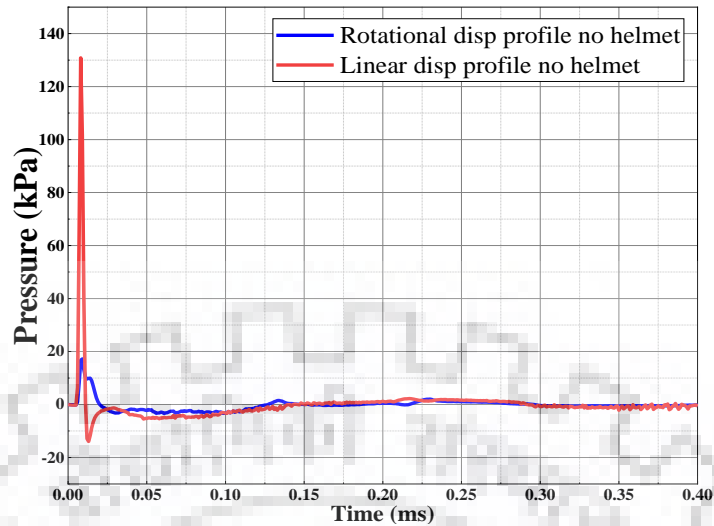


Figure 36: Pressure variation with linear and rotational displacement profile inputs.

The pressure variation in case of linear displacement is shown in *Figure 37* at the time of peak pressure. We can see here the coup and countercoup regions. The impactor strikes the front part of head so there we observed positive pressure (coup region) and opposite to that negative pressure region (countercoup).

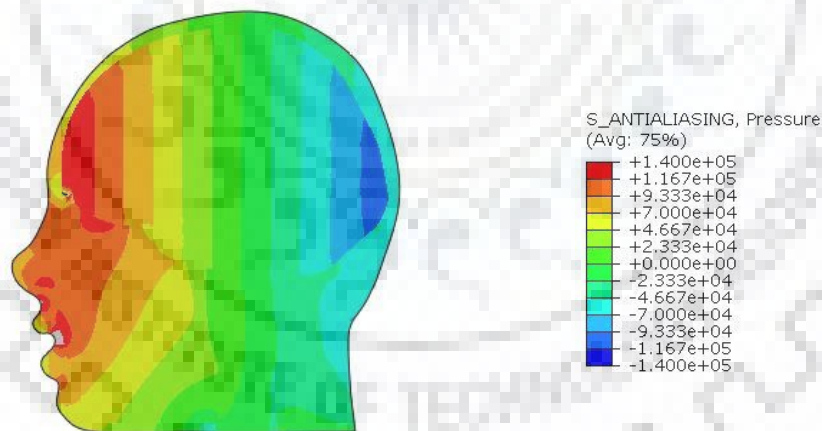


Figure 37: Pressure variation inside brain at the time of impact in case of linear displacement (pressure in Pa).

Variation of pressure profile with linear and angular displacement input in case of with helmet is shown in *Figure 38*. Maximum peak pressure is 120 kPa in this case which is less than without helmet case. This is possible due to foam pad absorbs the impact energy. Here we can see there are more fluctuations in pressure profiles due to use of foam.



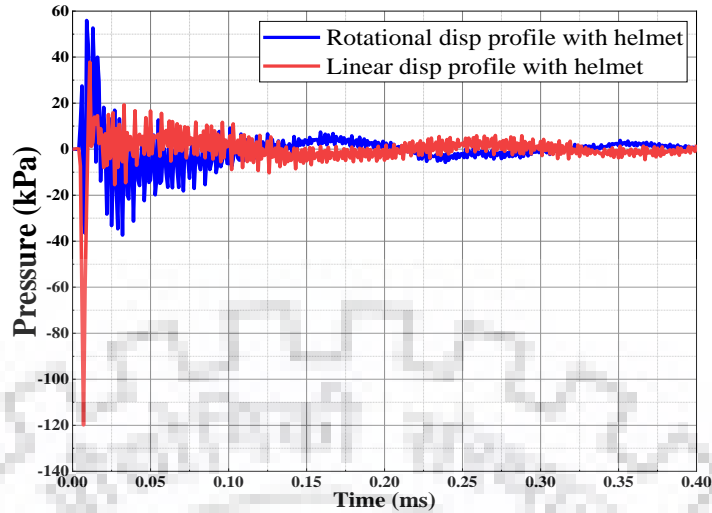


Figure 38: Pressure variation in case of with helmet.

In case of rotational displacement input profiles maximum principal stress variation in frontal part is shown in *Figure 39* with and without helmet. SEA 180 filter was used to extract the with helmet profile of stress. We observed that maximum principal stress in case of helmet was significantly higher than no helmet case. But we should note that this is comparable less stress than linear displacement input profiles.

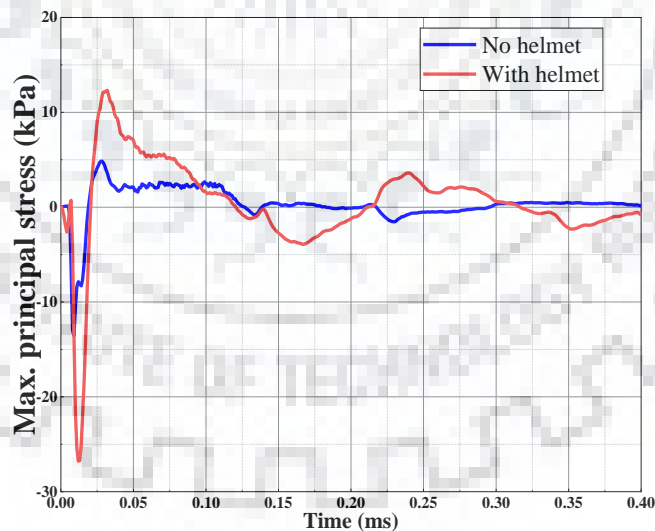


Figure 39: Max. principal stress variation in frontal part of brain.

We have the following observations by comparison of various brain responses in case of with and without helmet:

- (i) To study injury mechanisms, it is best to focus on brain reaction to complex inputs of linear and angular acceleration.

(ii) Angular acceleration is also important parameter in assessment of brain injury because it produces shear strain which deforms the brain, so linear and angular acceleration both should be considered to study the local brain deformation.

(iii) After initial phase shear strain in case of helmet is higher than no helmet case due to large peak angular acceleration.

(iv) Peak pressure rise is due to linear acceleration. Maximum principal stress is more in with helmet case when we apply rotational displacement profile, but it is significantly less than linear displacement case.

(v) If we apply these profiles independently i.e. linear and rotational profiles, on superposition of result we get same result as both profiles applied combined.

#### 5.4 Simulations on GHBMC full body model

To study the comparison of results between 2D and 3 D model we used GHBMC models which gives complete biofidelitic response of human body. The model was used to identify the response of brain during impact with helmet and no helmet. The impact speed was kept 3 m/s to compare the results with previous study. We modeled impactor with shell elements and adjusted the thickness to give total mass 17.3 kg. We kept back fix in two perpendicular directions of impact by applying constraint in Ls dyna (*Figure 40*). Because impact is a short duration incident so simulation time is taken as 15 ms. This took 4 hours with 32 cores using MPP solvers. There is some distance initially between impact and head before impact.



Figure 40: GHBMC model no helmet front impact.

ACH helmet was mounted on this model in Hypermesh and imported back in Ls dyna. The helmet shell is modeled as isotropic material and foam as hyper elastic material, LOW\_DENSITY\_FOAM model is chosen for this purpose in Ls dyna. Boundary conditions are same as previous case. Tied constraint was used between shell and foam due to no relative displacement.

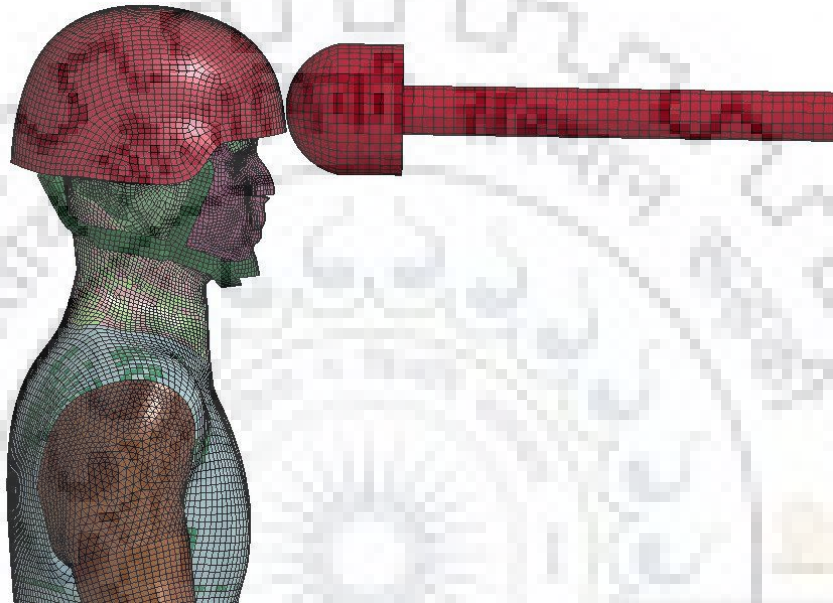


Figure 41: GHBMC model front impact with helmet.

Different contact definition used in this model are given in table-5. There is contact between solid elements of foam and shell element of skin of head so soft formulation is used in contact definitions.

**Table 5: Contact definitions for helmeted GHBMC model**

Tied constraint between foam pads and helmet inner surface (defined by segment ids) *CONTACT_TIED_SURFACE_TO_SURFACE
Contact between helmet shell and impactor (defined by part ids) * CONTACT_AUTOMATIC_SURFACE_TO_SURFACE
Contact between foam pad and head skin * CONTACT_AUTOMATIC_SURFACE_TO_SURFACE
Contact between chin strap and face skin * CONTACT_AUTOMATIC_SURFACE_TO_SURFACE
Contact between helmet and strap (defined using node and part ids) *CONSTRAINT_NODE_TO_SURFACE

## 5.4 Simulation results for GHBMC full body model

We tracked different profiles i.e. linear acceleration, rotational acceleration, pressure, contact forces, shear strain etc. to compare both cases of with and without helmet and show the effect of helmet on injury reduction.

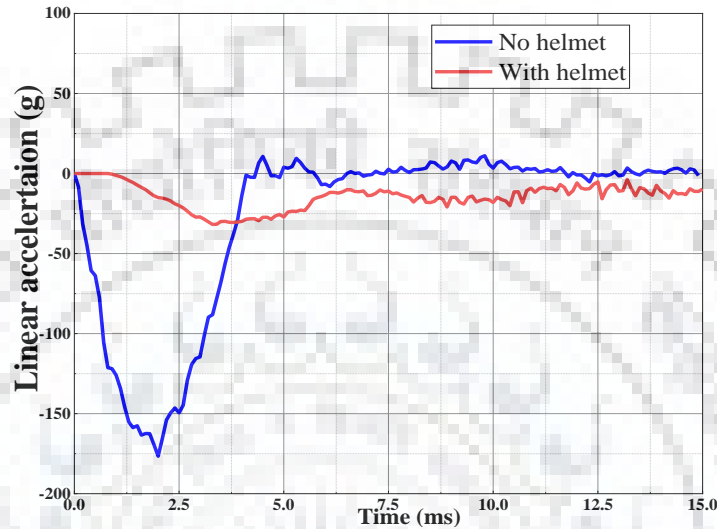


Figure 42: Linear acceleration comparison of with and without helmet.

Here also we can see the significant reduction of linear acceleration in case of with helmet (*Figure 42*). Hence we can see in figure that impact duration was increased in helmeted head. But the rotational acceleration in case of helmet increases. Peak of rotational acceleration is delayed due to compression of foam pad (*Figure 43*). Here we have allowed sliding between head and helmet. Initial small peak of acceleration in fig (b) is possibly due to chin strap contact.

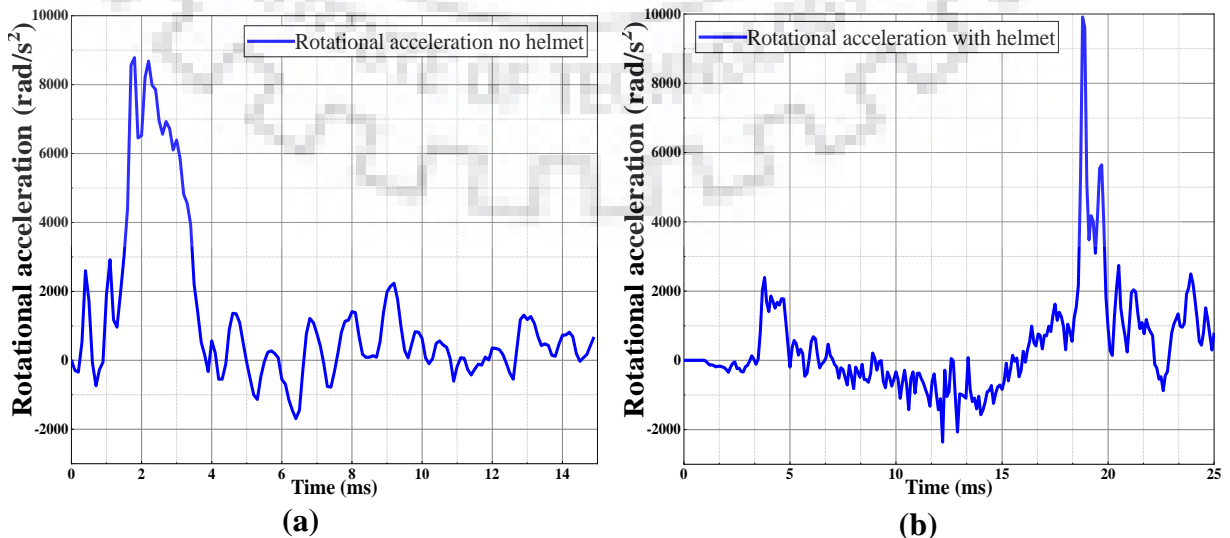


Figure 43: Rotational acceleration profiles (a) no helmet (b) with helmet during GBBMC model impact simulation

Albert I. King et. al. (2003) [31] also mentioned higher rotational acceleration in case of helmet during frontal impact. In 4 out of 9 different foam material helmet, rotational acceleration was more with helmet (*Figure 44*).

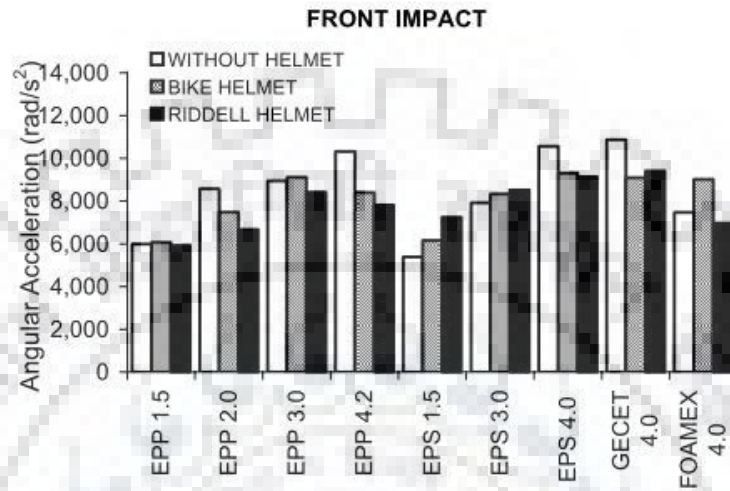


Figure 44: Comparison of angular acceleration with and without a bike helmet [31].

We can see that impact force on the skull is reduced significantly with the use of helmet hence helmet protects from skull fracture (*Figure 45*). Svein Kleiven [32] also told that most traumatic brain injuries caused due to skull fracture because higher impact stresses produced during high velocity impact. It is mentioned that oblique impact is more deleterious than frontal impact. Hence to mitigate the chances the skull fracture it is very necessary to use proper foam pad material in helmet. Pad reduces the peak impact force and increases impact duration.

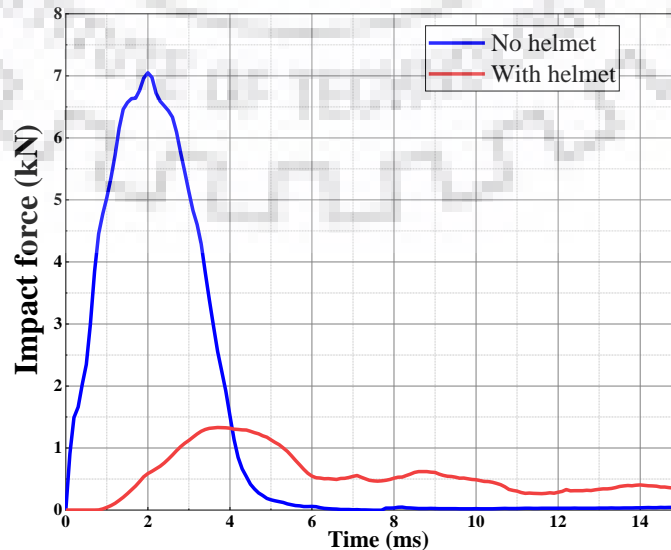


Figure 45: Impact forces on skull with and without helmet.

## 5.5 Summery

In this chapter we have discussed the effect of helmet on brain injury by assessment of various parameters. With the help of 2D model and Hybrid III dummy we presented the comparative study of linear and rotational acceleration which are considered as root cause of brain injury. We have found that helmet protect against linear acceleration produced injury by reducing peak acceleration, impact duration, peak impact force and intracranial pressure in the brain but rotational acceleration is increased probably due to added mass. Rotational acceleration increases shear strain inside brain because of low shear modulus of brain tissues. Various contact definitions during the simulation of GHBMC model plays an important role, so there are specially mentioned in the table. In helmeted case during GHBMC model simulations a delayed peak acceleration is found due to foam compression and due to same cause impact force profile becomes wider.



### CONCLUSION AND FUTURE SCOPE

---

We developed a 2 dimensional element and validated it with literature to investigate the effect of various types of impact loading conditions. In addition, the constructed model was used to determine rational parameters of elements of personal protection of the head. A comparative study has been presented between with and without helmet impact case. We have the following conclusions from our study.

1. Brain injury is related to local deformation response of brain and independent of global input to the head.
2. Linear and angular accelerations are responsible for different types of injury, so none of them can be ignored while studying brain injury.
3. Helmet mitigates the linear acceleration induced injury and reduces the chances of skull fracture but it increases the rotational acceleration which leads to diffuse axonal injury (DAI). So use of helmet is necessary but some modifications are required to reduce DAI.
4. Bulk modulus of brain tissues is 5 to 6 times higher than shear modulus so it mainly deforms due to shear stresses which are caused by rotational acceleration.
5. Different types of foam materials can be used for reduction of both linear and angular acceleration induced injury.

The studies conducted were simulated for understanding the fundamental mechanics of impact loading condition. To consolidate our claim of helmet is dangerous in case of rotational acceleration some future studies are needed. These are mentioned below

1. In two dimensional model we have used tied constraint between all interfaces, in future these can be set as internal sliding for more realistic simulations.
2. We have not considered the soft foam layer inside helmet, only hard foam layer is used. Because soft foam works as comfort linear. These can be added to increase energy absorption in helmet but the volume and inertia of helmeted head will increase due to distribution of mass.

3. We have studied only low velocity impact with velocity 3 m/s. As shown in various research papers that the response of helmeted head changes very drastically, so we need to verify our result with velocities 5 and 7 m/s.
4. Effects of variation of thickness, shape and cross sectional area of the helmet padding have to be studied to establish the comprehensive conclusions on the energy absorption of the helmet pads.
5. To validate all our results some experimental work need to be done.





## REFERENCES

---

- [1]. Tanielian, T., and Jaycox, 2008, "Invisible Wounds of War," Technical Report.
- [2]. Courtney, A. C., and Courtney, M. W., 2009, "A Thoracic Mechanism of Mild Traumatic Brain Injury Due to Blast Pressure Waves," *Medical Hypotheses*, 72(1), pp. 76-83.
- [3]. Kleiven, S., Peloso, P., von Holst, H. (2002). The Epidemiology of Head Injuries in Sweden From 1987 to 2000. Submitted to *Journal of Injury Control and Safety Promotion*.
- [4]. Gennarelli, T.A. et al. (1982). Diffuse Axonal Injury and Traumatic Coma in the Primate. *Ann. Neurol.* 12, 564-574.
- [5]. Melvin, J. W., Lighthall, J. W., and Ueno, K. (1993). "Brain injury biomechanics," in *Accidental Injury*, eds A. M. Nahum, and J. W. Melvin (New York: Springer-Verlag), 269–290.
- [6]. Shreiber, D. I., Bain, A. C., and Meaney, D. F. (1997). "In vivo thresholds for mechanical injury to the blood-brain barrier," in 41<sup>st</sup> Stapp Car Crash Conference (Warrendale, PA: Society of Automotive Engineers).
- [7]. Mertz, H. J., Prasad, P., and Irwin, A. L. (1997). "Injury risk curves for children and adults in frontal and rear collisions," in *Proceedings of the 41<sup>st</sup> Stapp Car Crash Conference* (Warrendale, PA: Society of Automotive Engineers).
- [8]. Ganpule, S., Gu, L., Alai, A., and Chandra, N., 2011, "Role of Helmet in the Mechanics of Shock Wave Propagation under Blast Loading Conditions," *Computational Methods Biomech Biomed Engin*, pp. 1-12.
- [9]. Lee, M.C., Melvin, J.W., Ueno, K. (1987). Finite element analysis of traumatic subdural hematoma. In *Proceedings of the 31st Stapp Car Crash Conf.*, SAE Paper No. 872201, Society of Automotive Engineers.
- [10]. Chu. et al. (1995). Computational analysis of head impact response under car crash loadings, in: 39th Stapp Car Crash Conf, Society of Automotive Engineers, SAE Paper No. 952718, pp. 425-438.
- [11]. Gilchrist MD, O'Donoghue D, Horgan TJ. A two-dimensional analysis of the biomechanics of frontal and occipital head impact injuries. *International Journal of Crashworthiness*. 2001 Jan 1;6(2):253-62.

- [12]. Lee, M.C., Melvin, J.W., Ueno, K. (1987). Finite element analysis of traumatic subdural hematoma. In Proceedings of the 31st Stapp Car Crash Conf., SAE Paper No. 872201, Society of Automotive Engineers.
- [13]. Zhou, C. et al. (1995). A new model comparing impact responses of the homogeneous and inhomogeneous human brain, in: 39th Stapp Car Crash Conf., Society of Automotive Engineers, 121-137.
- [14]. Zhang, L. et al. (2001a). Comparison of Brain Responses Between Frontal and Lateral Impacts by Finite Element Modeling. *J. Neurotrauma*, 18 (1), 21-30.
- [15]. Holbourn, A.H.S. (1943). Mechanics of head injury. *Lancet* 2, October 9, pp. 438-441.
- [16]. F. J. Unterharnscheidt, "Translational versus rotational acceleration: animal experiments with measured inputs," 1971.
- [17]. Gennarelli, T.A., Thibault, L.E., Ommaya, A.K. (1972). Pathophysiological Responses to Rotational and Translational Accelerations of the Head, SAE Paper No. 720970, in: 16th Stapp Car Crash Conf., Society of Automotive Engineers, pp. 296-308.
- [18]. Hodgson, V.R., Thomas, L.M. (1979). Acceleration induced shear strains in a monkey brain hemisection. SAE Paper No. 791023, in: 23rd Stapp Car Crash Conf., Society of Automotive Engineers.
- [19]. Hardy WN, Foster CD, Mason MJ, Yang KH, King AI, Tashman S. Investigation of head injury mechanisms using neutral density technology and high-speed biplanar X-ray. SAE Technical Paper; 2001 Nov 1.
- [20]. Hardy WN, Mason MJ, Foster CD, Shah CS, Kopacz JM, Yang KH, King AI, Bishop J, Bey M, Anderst W, Tashman S. A study of the response of the human cadaver head to impact. *Stapp car crash journal*. 2007 Oct;51:17.
- [21]. Bayly, P.V., Massouros, P.G., Christoforou, E., Sabet, A. and Genin, G.M., 2008. Magnetic resonance measurement of transient shear wave propagation in a viscoelastic gel cylinder. *Journal of the Mechanics and Physics of Solids*, 56(5), pp.2036-2049.
- [22]. Levadnyi, Ievgen, Jan Awrejcewicz, Yan Zhang, Márcio Fagundes Goethel, and Yaodong Gu. "Finite element analysis of impact for helmeted and non-helmeted head." *Journal of medical and biological engineering* 38, no. 4 (2018): 587-595.
- [23]. Post, A., Oeur, A., Hoshizaki, B., & Gilchrist, M. D. (2013). Examination of the relationship between peak linear and angular accelerations to brain deformation metrics in hockey helmet impacts. *Computer methods in biomechanics and biomedical engineering*, 16(5), 511-519.
- [24]. Rashid, B., Destrade, M., Gilchrist, M.D., 2012. Mechanical characterization of brain tissue in compression at dynamic strain rates. *J. Mech. Behav. Biomed. Mater.* 10,23–38.

- [25]. Gibson, L.J. Cellular Solids: Structure and Properties- Second edition. Cambridge, UK : Cambridge University Press, 1997.
- [26]. 6. Livermore Software Technology Corporation. LS-Dyna Keyword User's Manual, Version 971. 2007. pp. 226-227, 314.
- [27]. Fitek, John, and Erin Meyer. Design of a helmet liner for improved low velocity impact protection. No. NATICK/TR-13/016. ARMY NATICK SOLDIER RESEARCH DEVELOPMENT AND ENGINEERING CENTER MA, 2013.
- [28]. Moss, William C., and Michael J. King. Impact response of US Army and National Football League helmet pad systems. No. LLNL-SR-464951. LAWRENCE LIVERMORE NATIONAL LAB CA, 2011.
- [29]. Mohan, Pradeep, Dhafer Marzougui, and Cing-Dao Kan. Development and validation of hybrid iii crash test dummy. No. 2009-01-0473. SAE Technical Paper, 2009.
- [30]. GHBMC User Manual: M50 Detailed Pedestrian Version 1.5 for LS-DYNA.
- [31]. King, Albert I., et al. "Is head injury caused by linear or angular acceleration." IRCOBI conference. Vol. 12. Lisbon, Portugal, 2003.
- [32]. Kleiven, Svein. "Why most traumatic brain injuries are not caused by linear acceleration but skull fractures are." *Frontiers in bioengineering and biotechnology* 1 (2013): 15.